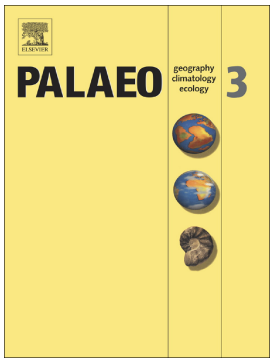

Permo-Triassic detrital records of South China and implications for the Indosinian events in East Asia

Lisha Hu, Peter A. Cawood, Yuansheng Du, Yajun Xu, Chenghao Wang, Zhiwen Wang, Qianli Ma, Xinran Xu

PII: S0031-0182(17)30351-6
DOI: doi: 10.1016/j.palaeo.2017.06.005
Reference: PALAEO 8321

To appear in: *Palaeogeography, Palaeoclimatology, Palaeoecology*

Received date: 2 April 2017
Revised date: 31 May 2017
Accepted date: 11 June 2017

Please cite this article as: Lisha Hu, Peter A. Cawood, Yuansheng Du, Yajun Xu, Chenghao Wang, Zhiwen Wang, Qianli Ma, Xinran Xu , Permo-Triassic detrital records of South China and implications for the Indosinian events in East Asia, *Palaeogeography, Palaeoclimatology, Palaeoecology* (2017), doi: 10.1016/j.palaeo.2017.06.005

Permo-Triassic detrital records of South China and implications for the Indosinian events in East Asia

Lisha Hu[1, 2, 3], Peter A Cawood[4, 5], Yuansheng Du[3*], Yajun Xu[3], Chenghao Wang[1], Zhiwen Wang[1], Qianli Ma[3], Xinran Xu[6]

1. Collage of Marine Geosciences, Ocean University of China, 238 Songling Road, Qingdao 266100, PR China

2. Key Laboratory of Submarine Geosciences and Prospecting Technology, Ministry of Education, China, 238 Songling Road, Qingdao 266100, PR China

3. State Key Laboratory of Biogeology and Environmental Geology, China University of Geosciences, Wuhan 430074, China

4. School of Earth, Atmosphere and Environment, Monash University, Clayton, Victoria, Australia,

5. Department of Earth Sciences, University of St. Andrews, Saint Andrews, UK

6. Institute of Geology and Geophysics, University of Chinese Academy of Sciences, Beijing 100029, PR China

*Corresponding author. Tel.: +86 13971241916; fax: +86 27 67885151.

E-mail address: duyuansheng126@126.com (Y. Du)

Abstract

Provenance analyses of Lower to Middle Triassic strata from the Greater Youjiang Basin along with the Permian strata of Hainan Island, provide a record of the collisional assembly of the South China Craton and Indochina Block and their incorporation into Asia. Detrital zircons from Lower and Middle Triassic samples show similar overall age spectra ranging from Archean to Triassic with major age groups at 300-250 Ma, 480-420 Ma, and 1200-900 Ma, as well as at 400-300 Ma in one Triassic sample. Permian siltstones from Hainan Island, to the southeast of the Greater Youjiang Basin, record different age spectra with major age groups at 400-300 Ma and 530-420 Ma and subordinate components at 1200-900 Ma and 1900-1700 Ma. These age data in combination with available paleocurrent data and regional geological relations suggest that Precambrian detrital zircons were derived from the Precambrian basement or recycled from the overlying early Paleozoic sedimentary

rocks that contain Precambrian detritus. Early Paleozoic detrital zircons were derived from igneous rocks in the South China Craton. Devonian-Triassic detrital zircons in the Triassic strata were likely sourced from coeval magmatic activity related to closure of Paleo-Tethys branch ocean that lay to the southwest, whereas 400-300 Ma detrital zircons in the Permian siltstones of Hainan Island were likely derived from a Paleozoic magmatic arc source that extended along the eastern-southeastern margin of China from Hainan Island to Japan in response to subduction of the Paleo-Pacific oceanic crust.

Detrital zircon, trace element, and sandstone modal data for Permo-Triassic strata from the Greater Youjiang Basin indicate that the basin evolved from a trailing-edge passive margin setting to a peripheral foreland basin during closure of the Paleo-Tethys Ocean and collision between Indochina and South China. The initiation time of the foreland basin decreases from southeast to southwest across the basin, probably reflecting oblique collision. In contrast, the Permian strata on Hainan Island record a provenance history distinct from the Greater Youjiang Basin, which is related to late Paleozoic to Mesozoic subduction of the Paleo-Pacific Plate beneath South China.

Keywords: Greater Youjiang Basin; Hainan Island; Paleo-Tethys; Paleo-Pacific; Permian-Triassic orogeny

1 Introduction

A major phase in the assembly of Eurasia involved the accretion of the South China Craton (SCC) and Indochina Block onto pre-existing blocks in Asia during the Permo-Triassic Indosinian orogeny (Metcalfe, 2011; Wang et al., 2013a; Faure et al., 2014). This orogenic event was recorded in widespread igneous activity and metamorphic events, and a change in sedimentation patterns from deep marine to a shallow marine/terrigenous dominated environment in South China (e.g., Wang et al., 2013a). Orogenesis is inferred to be driven by the termination of subduction of the Paleo-Tethys Ocean and subsequence accretion of the South China and Indochina

blocks onto Eurasia (Lepvrier et al., 2008; Cai and Zhang, 2009; Zhao et al., 2012; Zhang et al., 2013; Zi et al., 2013; Faure et al., 2014; Faure et al., 2016; Halpin et al., 2016; Qiu et al., In Press), and/or by the subduction of the Paleo-Pacific Plate beneath the eastern-southeastern margin of the South China Craton (Li and Li, 2007; Li et al., 2012; Hu et al., 2015a; Li et al., In Press).

There is a succession of mid-Paleozoic to early Mesozoic sedimentary rocks in the southwest to south portion of the craton (A, B and C areas in Fig. 1). They provide a record of the break-up history of the craton from the northern margin of Gondwana, associated with the opening of the Paleo-Tethys, the drifting of the craton across the ocean and its accretion onto Eurasia, as well as the collision between the South China and Indochina blocks (Zeng et al., 1995; Yang et al., 2012a; Lehrmann et al., 2014). The succession has traditionally been broken into a number of different basins (e.g. Youjiang, Pingxiang and Qinfang basins) separated by faults (e.g. Pingxiang-Nanning Fault) (BGMRGR, 1985; Meng et al., 2002). However, the bounding faults truncate rock units along the inferred basin margins, implying that they represent an imposed structural boundary and did not constitute the basin edge during sediment accumulation. In combination with continuity of sedimentary facies and similar detrital provenance of the Triassic units across the fault boundaries (e.g. Yang et al., 2012a; Hu et al., 2014, 2015a, this study), we consider the Devonian to Triassic strata in southwest China (Youjiang, Pingxiang-Chongzuo and Qinfang areas in Figure 1) accumulated in a single basin, here termed the Greater Youjiang Basin, as the traditional Youjiang Basin constitutes the major component of this expanded succession. The present day disruption of the Greater Youjiang Basin into the three currently recognized basins likely reflects Mesozoic northeast trending sinistral strike-slip faults and thrusts (Zhang and Cai, 2009; Cai, 2013) that in part bound and disrupt the Greater Youjiang Basin. In this paper, we present new data on the sedimentation and provenance records of the Triassic succession in thePingxiang-Chongzuo area of the Great Youjiang Basin (B area in figure 1) and the Permian succession of Hainan Island, which lies to the southeast of the basin (D area in Figure 1). We combine this data with that from other time equivalent sequences

along the southern margin of the craton (A, C, E areas in Figure 1) to provide a regional context for the data and to illuminate sedimentary basin evolution and tectonic setting of the South China Craton during the Permian and Triassic.

2 Geological Setting

The South China Craton was formed through amalgamation of the Yangtze and Cathaysia blocks along the Jiangnan Orogen during the early to middle Neoproterozoic (Wang and Mo, 1995; Li et al., 2007; Cawood et al., 2013, In Press). The craton includes dispersed Archean, Paleoproterozoic and minor early Mesoproterozoic basement units (Gao et al., 1999; Greentree and Li, 2008; Xia et al., 2012). The Neoproterozoic units record the assembly of the craton and its subsequent stabilization (e.g., Li et al., 2002; Li et al., 2008; Yu et al., 2009; Zhao and Cawood, 2012). Early Paleozoic to Mesozoic sedimentary successions unconformably overlie Precambrian basement (Wang et al., 2013a and references therein). The craton underwent early Paleozoic and early Mesozoic orogenic events involving magmatic and metamorphic activity. Permo-Triassic successions are distributed mainly in the Greater Youjiang Basin, the Yong'an Basin, and along the Jiangshan-Shaoxing fault system, with limited exposure on Hainan Island. The Permian deposits in the Greater Youjiang Basin and along the Jiangshan-Shaoxing fault are dominated by carbonate and chert whereas those in the Yong'an Basin and Hainan Island are dominated by siliciclastic rock. Overlying Triassic successions are principally composed of siliciclastic rock units except for carbonate platform accumulation in the Youjiang and Pingxiang-Chongzuo areas of the Greater Youjiang Basin and along the Jiangshan-Shaoxing fault in the early Triassic (BGMRFP, 1985; BGMRGR, 1985; BGMRGP, 1988; BGMRHN, 1988).

2.1 Greater Youjiang Basin

The Greater Youjiang Basin extends across the Youjiang, Pingxiang-Chongzuo and Qinfang areas of South China (Fig. 1). The basin is bounded by the Ziyun-Danchi Fault to the northeast, by the Bobai-Cenxi Fault to the southeast, which separates it from the Yunkai Massif, and to the northwest by the Shizong-Mile Fault, and is

bounded to the southwest by the Babu suture zone (Fig. 1). The Greater Youjiang Basin was initiated in the Silurian in the Qinfang area by rifting of the Cambrian-Ordovician succession (Xu et al., In Press). The Devonian-Early Triassic deposits consist of clastic, siliceous and pelitic carbonate rocks and intercalated igneous rocks (Liang and Li, 2005). Turbiditic clastic detritus infilled the basin from the Early Triassic in the Qinfang and Pingxiang-Chongzuo areas and from the Middle Triassic in the Youjiang areas (Yang et al., 2012a; Hu et al., 2014). Late Paleozoic ultramafic-mafic rocks are distributed along the southern margin of the Greater Youjiang Basin and Triassic granites outcrop around the Qinfang area (Wu et al., 1999; Wu et al., 2002; Guo et al., 2004; Zhao et al., 2012).

In the Pingxiang-Chongzuo area (Fig. 1), basal Devonian strata of the Greater Youjiang Basin are unconformable on the Cambrian basement. The Devonian to Permian units are composed of siliciclastic rocks, chert and calcareous horizons with accumulation of carbonates on localized platforms within the basin (BGMRGR, 1985; Lehrmann et al., 2007b). The Lower Triassic strata consist of the Luolou, Nanhong and Beisi formations and are well developed around the Shangsi, Zaimiao and Mabiao areas (Figs. 2A, B). The Luolou Formation, lying in the north part of the Pingxiang-Chongzuo area, consists of thick limestone. This contrasts with the time equivalent lateral succession of the Nanhong Formation (Figs. 2B, 3), which is composed of grey siltstone and shale in its lower part, and thick-bedded sandstone interbedded with thin siltstone horizons in its middle and upper parts (Figs. 3, 4A, B, C). The Beisi Formation, which outcrops across the middle and southern parts of the Pingxiang-Chongzuo area, is another time-equivalent unit to the Nanhong Formation and is a carbonate dominated succession, but also contains interstratified dacitic volcanic rocks and tuffs in the middle part of this formation (Figs. 2A and 3; BGMRGR, 1985 and geological map of Pingxiang 1:250000). The Beisi Formation is conformably overlain by the Middle Triassic Banna and Lanmu formations (Fig. 3). The lower part of the Banna Formation consists of interstratified siltstone and limestone lenses, passing up into mudstone, siltstone and sandstone (Fig. 4H, I, J, K). The Lanmu Formation consists of interbedded siltstone, mudstone and fine sandstone

(Fig. 4M). Sedimentary structures developed within the units include parallel and cross-bedding (Figs. 4D, E, F, G, N, O). Paleocurrent data for the Nanhong Formation indicates sediment transport to the northwest (Fig. 2B; Liang and Li, 2005) whereas data for the Middle Triassic units is more complex with paleocurrent data indicating alternating flow to the northeast-northwest and south (Fig. 2A; Song et al., 2013).

2.2 Hainan Island

Hainan Island is located offshore from the South China mainland to the southeast of the Greater Youjiang Basin (Fig. 1). The island consists of a basement of early Mesoproterozoic igneous and sedimentary rocks and Neoproterozoic sedimentary units (BGMRGP, 1988; Yao et al., 2017), overlain by Paleozoic to Mesozoic strata (Xu et al., 2014b; Zhou et al., 2015). The Permian-Early Triassic units are sporadically distributed in the Jiangbian and Danzhou areas along the Changjiang-Qionghai Fault (Fig. 2C; BGMRGP, 1988).

The Permian sequence is unconformable on the Silurian succession and disconformable with the Carboniferous succession in the southwest of Hainan Island (BGMPGP, 1988). The Permian succession consists of grey siltstone, shale, and fine sandstone (Jiang et al.,1998; Long et al., 2007) interbedded with limestone lenses and chert. The radiolarian fossil *Pseudoalbaillella sp* is preserved in the chert layers (Long et al., 2007), as well as conodont fossils *Neogondolella sp*, *Sweetognathus whitei-Rabeignathus asymmetricus* similar to the *Aktastinian Sweetognathus whitei-Neogondonella bisselli* and sporopollen fossil *Parafusulina sp* (Tang et al., 1998). The Triassic succession is made up of conglomerate, sandstone and siltstone which are scattered across Hainan Island (BGMRGP, 1988). Paleozoic igneous rocks have a limited distribution whereas the Mesozoic igneous rocks are widespread on the island (Li et al., 2006; Chen et al., 2013; Wang et al., 2013c).

3 Sample setting and analysis methods

Three sections through the Lower to Middle Triassic successions in the Pingxiang-Chongzuo area were measured and sampled for detrital provenance analysis as well as two Permian siltstones from Hainan Island (Figs. 2 and 3).

Weathered surfaces were removed from samples prior to analysis. The Gazzi-Dickinson method was used to point count twenty-five sandstones, with 300-500 grains counted from each sample (see Data Set S1). Samples selected for geochemical analysis included five mudstone/siltstone from the Nanhong Formation, thirteen mudstone/siltstone from the Banna Formation and ten mudstone/siltstone from the Lanmu Formation (Date Set S1; Fig. 3). Major, trace and rare earth element (REE) analyses were carried out at the Laboratory of ALS Chemex (Guangzhou). Major elements were determined using X-ray fluorescence spectrometry (XRF) on fused beads with accuracy of analyses estimated to be ca. 1% (relative). Trace element and rare earth element (REE) analyses were determined using inductively coupled plasma atomic emission spectroscopy (ICP-AES) and inductively coupled plasma mass spectrometry (ICP-MS). The accuracy of analyses is estimated between 0.01-10 ppm depending on abundance of the different trace elements (Data Set S2).

Three sandstone samples of the Lower Triassic Nanhong Formation, one sandstone sample of the Middle Triassic Banna Formation, one sandstone sample of the Middle Triassic Lanmu Formation and two Permian siltstone samples from Hainan Island were collected for detrital zircon age analysis (Figs. 2C, 3). Zircons were separated from the samples using conventional density and magnetic separation techniques, then polished for back-scattered electron (BSE) and cathodoluminescence (CL) imaging on a JXA-8100 at the State Key Laboratory of Geological Processes and Mineral Resources (GPMR), China University of Geoscience (Wuhan). The detailed analytical procedure is described by Liu et al. (2010). U-Pb ages for the detrital zircons and trace elements were determined on an Agilent 7700a at GPMR, China University of Geoscience (Wuhan). The analytical procedure followed Yuan et al. (2004) and Liu et al. (2010). Off line selection, integration of background, analytic signals, time-drift correction and quantitative calibration for U-Pb dating were performed with ICPMSDataCal (Liu et al., 2010). Spot diameter was 32 μm. Errors on individual analyses are given at 1 sigma (Liu et al., 2010). All measurements were normalized relative to standard zircons 91500 and GJ-1. Standard silicate glass NIST SRM610 was used to calibrate the contents of trace elements (Liu et al., 2010).

Common Pb correction was not performed as U-Pb ages are concordant or nearly concordant. The average analytical error ranges from ca. ± 10% for light rare earth elements (LREE) to ca. ± 5% for the other REE. Zircon U-Pb age concordance is defined as 100 × (1-abs ($^{206}Pb/^{238}U$ Age-$^{207}Pb/^{235}U$ Age)/$^{206}Pb/^{238}U$. Age and probability density plots were calculated using the Isoplot program 3.0 (Luding, 2003). In order to reduce the effects of Pb loss, ages older than 1000 Ma were based on $^{207}Pb/^{206}Pb$ ages whereas for younger analyses they were based on $^{206}Pb/^{238}U$ ages (Compston et al., 1992). LA-ICP-MS detrital zircon age data for the analyzed detrital zircons are listed in the Data Set S3.

4 Results

4.1 Sandstone petrography and modal analysis

Framework grains in all analyzed samples are angular to extremely angular with poor to moderate sorting (Fig. 5). Detrital grains are 0.2-0.5 mm in length for the Lower Triassic sandstone and around 0.1 mm for the Middle Triassic samples. Most grains in the Permian siltstones on Hainan Island are less than 0.07 mm and are unsuitable for point-counting. For samples from the Pingxiang-Chongzuo area, point counted framework grains are quartz (monocrystalline and polycrystalline), feldspar (invariably plagioclase), and lithic fragments (sedimentary, volcanic and metamorphic fragments). The sedimentary fragments include clastic grains, limestone and chert. Volcanic fragments are dominated by lathwork, felsic and vitric, and metamorphic fragments are mainly composed of sericite, chlorite and epidote.

The major detrital components of the Lower Triassic samples are monocrystalline quartz (62.1%-79.7%; average 72.0%) and unstable lithic fragment (generally sedimentary or volcanic 17.1%-36.3%; average 22.7%), with a small amount of plagioclase feldspar (0-3.73%; average 1.5%) (Date Set S1). The Middle Triassic siltstones/sandstones contain a greater proportion of lithic fragment (25.1%-45.4%; average 36%) and feldspar (0.63%-7.43%; average 5%), and less quartz (47.1%-73%; average 59%) than the Lower Triassic samples. The proportion

of volcanic fragments shows an overall increase from the Lower Triassic to Middle Triassic samples. All the counted samples are plotted on the Q-F-L and Qm-F-Lt diagrams and fall within or close to the recycled-orogen field (Figs. 6A and B), whereas they lie along or close to the Lv-Ls tie and largely in arc orogen source on the Qp-Lv-Ls diagram (Fig. 6C).

4.2 Whole rock geochemistry

The SiO_2 content of the Lower Triassic samples (average 63.7%) is slightly higher than that of the Middle Triassic samples (average 60.4%). All samples contain moderate Al_2O_3 (12.6%-19.7%) and Fe_2O_3 values (4.28%-7.79%). Alkali elements Na_2O, K_2O and CaO in the Lower-Middle Triassic samples are 0.09 %-1.48 %, 1.45%-4.44% and 0.15%-5.5%, respectively.

All the Triassic samples show similar chondrite-normalized rare earth element and primitive-normalized trace element distribution patterns, with light REE enrichment (LREE/HREE ratio of 7.01-10.5 for the Lower Triassic samples and 6.57-7.7 for the Middle Triassic samples), a negative Eu anomaly, depletion in high field strength elements (Nb, Ta and Ti), and enrichment in large ion lithophile elements (Th, U and Ba), similar to those of the upper continental crust (Figs. 7A and B; Taylor and McLennan, 1985; Sun and McDonough, 1989). Furthermore, the Lower Triassic samples contain higher rare earth element contents (REE = 161-250 ppm, average 205 ppm) than that of the Middle Triassic samples (REE = 130-186 ppm, average 159 ppm). The Lower and Middle Triassic samples have similar Th/U ratios of 4.22-5.13 and 4.32-5.07, respectively, whereas the Lower Triassic samples contain high Th/Sc and Zr/Sc values of 0.98-1.14 (average 1.16) and 7-19.2 (average 11.7) than that of the Middle Triassic samples (0.57-0.87; average 0.66; 7.25-15.1; average 9.8) (Figs. 7C and D; Data Set S2).

4.3 Detrital zircon ages

Detrital zircons from the Triassic strata in the Greater Youjiang Basin and the Permian units on Hainan Island are transparent to semi-transparent, subhedral to occasionally rounded. Lengths of the zircons are ~100 μm for the Lower Triassic samples and 50-100 μm for the Permian and Middle Triassic samples. Most analyzed

zircon grains display oscillatory zoning and sector structure in cathodoluminescence (CL) images and a small portion show core-rim and homogeneous structures (Fig. S1). Of a total 515 analyses on 514 zircon grains from seven sandstones, 480 analyses yielded concordant ages (Date Set S3). Most of the analyzed zircons contain high Th/U ratio (≥ 0.1; Date Set S3). All analyses are plotted on concordia diagrams (Fig. S2), whereas only analyses with concordance more than 90 are incorporated in the combined probability density plot and histogram (Fig. 8) and discussed in the following sections.

One hundred and fifteen analyses were conducted on 114 zircons of the Permian siltstones from Hainan Island (15LJ15, 15LJ49) and 95 gave concordant ages ranging from 2650 Ma to 216 Ma. Dominant age groups occur at 400-330 Ma, 520-420 Ma and subordinate age groups at 1200-900 Ma and 1900-1700 Ma.

Two hundred and forty U-Pb age analyses were conducted on 240 zircons from the Lower Triassic sandstone samples (BL-1, ZM4 and PM2), and 230 grains display concordance greater than 90% and range in age from 3652 Ma to 226 Ma. Sample BL1 from the Zaimiao section is dominated by age groups at 650-500 Ma, 1200-800 Ma, 1800-1200 Ma, with a subordinate age group at 460-420 Ma. Samples ZM4 from the Zaimiao section and PM2 from the Mabiao section contain similar age patterns with major age groups at 480-420 Ma, 1200-800 Ma but different subordinate age groups including at 300-220 Ma, 670-550 Ma, 900-700 Ma, 1800-1300 Ma and 2800-2000 Ma (Fig. 8).

One hundred and sixty analyses were conducted on 160 zircons of the Middle Triassic sandstones (PX20 and AZ20) and 155 analyses yield concordance greater than 90%. The two samples display age spectra that range from 2847 Ma to 237 Ma, with major age groups at 300-230 Ma, 1200-900 Ma and 900-700 Ma for sample AZ20, and at 300-230 Ma, 400-300 Ma, 480-420 Ma and 1800-1500 Ma for sample PX20.

5 Discussion

5.1 Provenance of the Permian and Triassic successions

The Lower and Middle Triassic samples from the Pingxiang-Chongzuo area are dominated by quartz and lithic fragments with little feldspar, and fall into the recycled orogen field on the QFL diagram (Figs. 6a and b; Dickinson and Suczek, 1979), coincident their high SiO_2 content (Data Set S2). REE and trace element patterns of samples are similar to upper continental crust, along with high Th/Sc and Zr/Sc ratios, indicating that detritus were sourced from felsic rocks (Figs. 7A-D). The presence of some lathwork volcanic fragments in the Triassic samples indicates an additional contribution from basaltic sources. On the basis of paleocurrents, which trend northwest in the Lower Triassic strata (Fig. 2b; Liang and Li, 2005) and north-northwest, south/southeast in the Middle Triassic succession (Fig. 2a; Song et al., 2013), potential source areas are the Yunkai Massif, Hainan Island and/or North Vietnam.

Detrital zircon spectra for the Permian siltstones from Hainan Island differ from the Lower-Middle Triassic sandstones from the Pingxiang-Chongzuo area of the Greater Youjiang Basin (Fig. 8). Devonian to Carboniferous (400-300 Ma) zircons are the dominant component of the Permian siltstones (14.7%-37.7%) whereas they are largely lacking from the Triassic samples, except for sample PX20, which contains 16.7% detritus of this age. The Triassic samples also contain Permian and Triassic detrital zircons (300-230 Ma; (Fig. 8). 5.1.1 Provenance of pre-Devonian detrital zircons

Precambrian detrital zircons (＞550 Ma) are preserved in all analyzed samples. They are the dominant age group in the Lower Triassic samples and Middle Triassic sample AZ20, but are subordinate to Phanerozoic age detritus in the Permian samples and Middle Triassic sample PX20 (Fig. 8). The Precambrian detrital zircons are euhedral to subhedral and under CL imaging display sector and oscillatory zoning and core-rim structure, suggesting derivation from multiple sources. Paleoproterozoic (ca. 1800) and Neoproterozoic (1200-900 Ma) magmatic rocks exposed in the Yunkai and Wuyi massifs to the southeast and east of the study area (Wang et al., 2011b; Wang et al., 2013b; Yao et al., 2017), together with at least some paleocurrent data indicating sediment transport to the west-northwest, argue for these massifs to have acted as

potential source areas (Figs. 2A and 2B; Liang and Li, 2005; Song et al., 2013). Reworking of the Neoproterozoic and early Paleozoic sedimentary successions in the Cathaysia Block and Hainan Island, provide another potential source for this age detritus. These older successions are dominated by detrital zircons with ages of 2000-1700 Ma and 1200-900 Ma (Yu et al., 2010; Xu et al., 2014b; Zhou et al., 2015; Yao et al., 2017). Detrital zircons with ages in the range 900 Ma to 700 Ma are a minor component in all samples (Fig. 8) and rocks of this age are widely distributed in the Jiangnan orogen (Li et al., 2008; Zhao and Cawood, 2012; Yin et al., 2013), and constitute the likely original source. However, in the Early Triassic, the Jiangnan orogen was submerged and detrital zircons of this age were probably derived from recycled material from the Yunkai Massif, which contains 900-700 Ma detrital zircons (Xu et al., 2014a). A minor component of the late Neoproterozoic detrital zircons (650-550 Ma) are present in the Lower Triassic samples, but primary magmatic sources of this age are absent from the South China Craton (including Hainan Island) and North Vietnam. Detrital zircons of this age are present in the early Paleozoic sedimentary units from the Yunkai Massif (Xu et al., 2014a), and this is considered as the probable source for this detritus.

Cambrian detrital zircons (530-470 Ma) are a major age group in the Permian samples from Hainan Island and an extremely rare component in the Triassic samples (1-4 grains) from the Greater Youjiang Basin (Fig. 8). Magmatic units on the island that have yielded a Sm-Nd age of 527 Ma (Ding et al., 2002) and the early Paleozoic sedimentary units in the Cathaysia and eastern Yangtze blocks, which contain Cambrian detrital zircons (Wang et al., 2010; Xu et al., 2014a), could be the potential sources of this age detritus. The rarity of 530-470 Ma detrital zircon in the Triassic samples possibly reflects the greater distance from the Greater Youjiang Basin to source areas than that of the samples on Hainan Island.

The 470-420 Ma detritus in analyzed samples are subhedral to euhedral with oscillatory zoning and Th/U ratios of more than 0.1, suggesting derivation from first-cycle source and corresponding with widespread mid-Paleozoic magmatic orogenic events in the Cathaysia Block (Peng et al., 2006; Wang et al., 2007; Wang et

al., 2011c; Chen et al., 2012).

5.1.2 Provenance of Devonian-Triassic Triassic detrital zircons

Devonian-Carboniferous (400-300 Ma) detrital zircons are a major age group in all the Permian siltstones from Hainan Island but are only present in one sample (PX20) from the Pingxiang-Chongzuo area (Fig. 8). Most 400-300 Ma zircons are subhedral to euhedral, with well-developed oscillatory zoning and Th/U ratio more than 0.1, suggesting minimal transport from magmatic sources. Potential source rocks are exposed along the southwestern and southeastern margins of the South China Craton. Igneous rocks on Hainan Island are a probable source for the Devonian and Carboniferous detritus in the Permian samples. Granite on the island has yielded a Devonian age of 368 ± 5 Ma (SHRIMP zircon U-Pb age, Ding et al., 2005) whereas volcanic rock has yielded Carboniferous ages of 345 ± 4 Ma (LA-ICP-MS zircon U-Pb age, Chen et al., 2013) and 328 Ma (whole rock 39Ar/40Ar age, He et al., 2016).

Mid-Paleozoic igneous rocks on Hainan Island are however, an unlikely source for the 400-300 Ma detritus in the Middle Triassic sample PX20. This is because the Yunkai Massif likely acted as a topographic barrier that prevented transport of detritus from the southeast Hainan Island since the Late Permian as well the lack of detritus of this age from the intervening Late Permian-Triassic strata in the Qinfang area (Liang and Li, 2005; Liang et al., 2013; Hu et al., 2015b). The Jinshajiang-Ailaoshan-Song Ma-Babu zone, along the southern-southwestern margin of the Greater Youjiang Basin (Fig. 1), is a more likely source, and is consistent with the paleocurrent data indicating flow to northeast. The suture zone contains Devonian to Carboniferous (400-300 Ma) igneous rocks and tuffs, related to the Paleo-Tethys branch ocean (Fig. 9; Zhong et al., 1998; Wu et al., 1999; Guo et al., 2004; Jian et al., 2009a; Jian et al., 2009b; Huang, 2013; Halpin et al., 2016; Nie et al., 2016). Furthermore, the majority of the Greater Youjiang Basin formed a bathymetric high in the Permian and hence would have prevented transport of detritus from the southwest of the Greater Youjiang basin towards Hainan Island (Huang et al., 2013).

Syn-orogenic Permo-Triassic zircons (300-230 Ma with peak age at ~250 Ma)

are the dominant age group in the Middle Triassic samples (20.8%-23.1%, Table S-1), as well as a minor component in the Lower Triassic samples (2.8%-6.9%, Fig. 8). These detrital zircons are euhedral to subeuhedral, with high Th/U ratios and oscillatory zoning, suggesting a magmatic origin and short transport distance from source areas (Belousova et al., 2002). Suitable sources are coeval magmatic rocks distributed along the southern margin of Guangxi Province in Napo-Pingxiang-Dongxi-Yunkai and Hainan Island and North Vietnam (Fig. 9; Li and Li, 2007; Qin et al., 2011; Hu et al., 2012; Jia et al., 2012; Qin et al., 2012; Roger et al., 2012; Halpin et al., 2016), which is consistent with the north-directed paleocurrent data. Permian-Triassic igneous units on Hainan Island are considered an unlikely source as the intervening Late Permian-Triassic units in the Qinfang area contain only a small amount of 300-200 Ma detritus (0.4%-4.3%) in comparison to the Middle Triassic strata in the Youjiang and Pingxiang-Chongzuo areas (21.8%-21.9%, Figs. 10 and 11). A single zircon grain in the Permian sample 15LJ15 yielded an age of ca. 216 Ma, younger than the depositional age. In CL, the grain is black and has a Th/U ratio of 0.96, and is interpreted to reflect post-depositional alteration (Belousova et al., 2002) perhaps related to the widespread Late Triassic tectonic events in the South China Craton (e.g. Li and Li, 2007).

5.2 Permo-Triassic paleogeographic evolution of Southwest China

The composition and provenance of the Permo-Triassic sedimentary units in the Greater Youjiang Basin helps constrain the paleogeographic evolution of South China and its role in the assembly of Asia. They provide a record of the break-up history of the South China Craton from the northern margin of Gondwana, associated with the opening of the Paleo-Tethys, the drifting of the craton across the ocean and its accretion onto Eurasia, as well as the collision between the South China and Indochina blocks (e.g., Cocks and Torsvik. 2013; Metcalfe. 2013). Moving up section, the Lower Triassic to Middle Triassic samples in the basin display an overall increase in the proportion of feldspar, lithic fragments and Devonian or younger (<400 Ma) detrital zircons (e.g., Figs. 10-11), whereas there is a decrease in the proportion of monocrystalline quartz, SiO_2 contents, REE contents, and Th/Sc and Zr/Sc ratios

(Yang et al., 2012a; Hu et al., 2015b, this study). This likely indicates an increasing component of the first-cycle detritus up-section. Abundant syn-orogenic detrital zircons (300-240 Ma, 20.8%-23.1%, Table S-1) preserved in the Middle Triassic samples indicates widespread uplift and exhumation of the basin hinterland during the Indosinian orogeny.Sedimentary facies in the Greater Youjiang Basin record significant changes in the setting of South China over time. Devonian to late Paleozoic strata in the basin record the rift and drift history of South China from northern Gondwana during opening of the Paleo-Tethys (Zeng et al., 1995; Lehrmann et al., 2007a; Du et al., 2013). Shallowing of the basin and development of terrestrial facies, commencing in the Late Permian-Triassic is inferred to represent conversion to a foreland basin associated with collision between the South China and Indochina blocks (Cai and Zhang, 2009; Zhao et al., 2012; Faure et al., 2016). The timing of this conversion appears to be diachronous from southeast to southwest, occurring in the Late Permian in the Qinfang area, in the Early Triassic in the Pingxiang-Chongzuo area, and in the Middle Triassic in the Youjiang area (Fig. 9; Liang and Li, 2005; Yang et al., 2013 and this study; Hu et al., 2014; Hu et al., 2015b; Qiu et al., In Press, this study). Late Triassic units are limited to Qinfang area, and consist of a thick succession of inferred molasse sediments derived from source areas similar to that of the early-middle Triassic succession in the Greater Youjiang Basin (Hu et al., 2014). This evolving basin setting is supported by the cumulative proportion plot of the difference between the measured crystallization ages (CA) of individual zircon grains present within a sample and the depositional age (DA) of the sample (Fig. 12). The Late Permian samples plot in or close to the extension-related basin setting whereas the Triassic samples move progressively into the syn-orogenic field with decreasing depositional age (Cawood et al., 2012). Trace element data also indicate a change from extension to convergent settings between the Permian and Triassic samples (Fig. 7E). This evolving basin paleogeography is shown schematically in Figure 13.

5.3 Subduction of the Paleo-Pacific beneath the eastern-southeastern margin of the SCC

On the basis of seismic reflection profiles, the distribution of the

Devonian-Permian magmatic rocks, and detrital zircon chronology data from Japan and southeast China, Isozaki et al. (2010) and our group (Hu et al., 2015a) have proposed that the South China Craton extended farther to the east (including Japan) in the Paleozoic and Mesozoic (Cocks and Torsvik, 2013; Isozaki et al., 2014). This Greater Cathaysia Block was subsequently removed through multiple episodes of subduction erosion during the Mesozoic (Fig. 14; Isozaki et al., 2010; Isozaki et al., 2014; Aoki et al., 2015; Isozaki et al., 2015). Permian siltstones in Hainan Island comprise different detrital zircon age spectra and source areas with that of the Greater Youjiang Basin (section 5.1) and likely represent a remnant of this Greater Cathaysia Block. The 400-300 Ma detritus in the Permian samples of Hainan Island (29.5% this study) and in samples of the Yong'an Basin (21.9% in the Permian sandstone and 13.4% in the Triassic sample) (Figs. 10 and 11; Li et al., 2012; Liang et al., 2013; Hu et al., 2015a) were likely derived from an eastern magmatic arc source related to the subduction of the Paleo-Pacific plate beneath the eastern-southeastern margin of China (Li and Li, 2007; Li et al., 2012; Hu et al., 2015a). The Permian siltstone detrital zircon data along with the presence of Devonian-Permian magmatic units on Hainan Island are consistent with the proposal that the island represents the southwest extension of this Paleozoic to Mesozoic accretionary belt (Hu et al., 2015a). Permian detrital zircons (300-260 Ma) are common in the Permo-Triassic sandstones in the Yong'an Basin but absent in Hainan Island samples. This could be due to: 1) the Permian magmatic rocks are not exposed at this time on Hainan Island; 2) as the inferred southern-most extent of the subduction zone of the Paleo-Pacific, the Permian magmatic rock were not well developed on Hainan Island.

The contrasting provenance record of the Greater Youjiang Basin, the Yong'an Basin, and the Hainan Island region reflect the differing paleogeographic settings of these regions with respect to margins of the South China Craton and outboard oceanic realms (Figs. 9 and 14). During the Permo-Triassic, the Greater Youjiang Basin records the conversion from a passive margin setting facing the open-ocean Paleo-Tethys to the south to a foreland basin associated with collision between the South China and Indochina blocks. Whereas the Yong'an Basin and Hainan Island

region faced the Paleo-Pacific Ocean, which was being subducted beneath the eastern-southeastern margin of the South China Craton during the late Paleozoic to Mesozoic (Fig. 14).

6 Conclusions

(1) The Lower Triassic and Middle Triassic samples in the Pingxiang-Chongzuo area of the Greater Youjiang Basin display an overall increase in the proportion of feldspar, lithic fragments, and Devonian or younger (< 400 Ma) detrital zircons, as well as a decrease in the proportion of monocrystalline quartz, SiO_2 contents, REE contents, and Th/Sc and Zr/Sc ratios from the Lower Triassic to Middle Triassic samples. This likely indicates an increasing component of the first-cycle detritus up-section. These data in combination with available paleocurrent data and regional geological relations suggest that Precambrian detrital zircons were derived either from Precambrian basement or via reworking of early Paleozoic sedimentary rocks that contain Precambrian detritus in the South China Craton. Early Paleozoic detrital zircons were derived from early Paleozoic igneous rocks in the craton. Devonian-Triassic detrital zircons were likely sourced from syn-sedimentary magmatic activity related to opening of the Paleo-Tethys Ocean that lay to the southwest.

(2) Major detrital zircon age groups in Permian siltstone on Hainan Island are at 400-300 Ma, 530-470 Ma and 470-420 Ma and a few grains on 1900-1700 Ma and 1200-900 Ma. In combination with the regional geological data, the pre-Devonian detrital zircons are inferred to have been derived from similar sources to the Triassic samples in the Greater Youjiang Basin. However, Middle Paleozoic detrital zircons (400-300 Ma) were likely derived from a Paleozoic magmatic arc source that extended along the eastern-southeastern margin of China from Hainan Island to Japan that formed in response to subduction of the Paleo-Pacific Ocean.

(3) Integration of our data with that from contemporaneous strata and igneous rocks along the southern margin of the South China Craton suggest that the Greater Youjiang Basin in the Late Permian to Middle Triassic recorded the transition from an extension-related continental rift to drift basin succession to a contraction-related foreland basin sequence. This evolution of basin type was a consequence of closure of

the Paleo-Tethys Ocean and oblique collision and accretion of the South China and Indochina blocks onto Asia. In contrast, Hainan Island constituted the southwest part of a magmatic arc suture zone related to subduction of the Paleo-Pacific (Panthalassa) Plate beneath the eastern-southeastern margin of the South China Craton in the late Paleozoic to Mesozoic.

Acknowledgments

We thank three anonymous reviewers and editor-in-chief Professor Thomas Algeo for detailed comments which lead to significant improvements in the manuscript. The data for this paper are available as Data Sets S1-S3. Figures S1 and S2 and Table S-1 are in the supporting information Text S1. This work was supported by the National Natural Science Foundation of China (Grant No. 41602105, 41672106 and 41530966) and China Postdoctoral Science Foundation (Grant No. 2016M590655), the fundamental Research Funds for the Central Universities, Ocean University of China. Peter Cawood acknowledges support from the Australian Research Council grant FL160100168. We thank Zhaochu Hu and Tao He for their help with zircon LA-ICP-MS U-Pb dating.

References

Aoki, K., Isozaki, Y., Yamamoto, A., Sakata, S. and Hirata, T., 2015. Mid-Paleozoic arc granitoids in SW Japan with Neoproterozoic xenocrysts from South China: New zircon U–Pb ages by LA-ICP-MS. Journal of Asian Earth Sciences, 97, Part A: 125-135.

Belousova, E., Griffin, W., O'reilly, S.Y. and Fisher, N., 2002. Igneous zircon: trace element composition as an indicator of source rock type. Contributions to Mineralogy and Petrology, 143(5): 602-622.

BGMRFP, 1985. Regional Geology of Fujian Province (in Chinese). Geological publishing House, Beijing: 1-671.

BGMRGP, 1988. Regional Geology of Guangdong Province (in Chinese). Geological Publishing House,Beijing: 1-941.

BGMRGR, 1985. Regional Geology of Guangxi Zhuang Autonomous Region (in Chinese). Geological Publishing House, Beijing: 1-853.

BGMRHN, 1988. Regional Geology of Hunan Province (In Chinese). Geological publishing House,

Beijing: 169-225.

BGMRYP, 1990. Regional Geology of Yunnan Province (in Chinese). Geological publishing House, Beijing: 1-736.

Bhatia, M.R. and Crook, K.A.W., 1986. Trace element characteristics of graywackes and tectonic setting discrimination of sedimentary basins. Contributions to Mineralogy and Petrology, 92(2): 181-193.

Cai, J.X., 2013. An Early Jurassic dextral strike-slip system in southern South China and its tectonic significance. Journal of Geodynamics, 63(63): 27-44.

Cai, J.X. and Zhang, K.J., 2009. A new model for the Indochina and South China collision during the Late Permian to the Middle Triassic. Tectonophysics, 467(1-4): 35-43.

Cawood, P.A., Hawkesworth, C. and Dhuime, B., 2012. Detrital zircon record and tectonic setting. Geology, 40(10): 875-878.

Cawood, P.A., Wang, Y., Xu, Y. and Zhao, G., 2013. Locating South China in Rodinia and Gondwana: A fragment of greater India lithosphere? Geology, 41(8): 903-906.

Cawood, P.A., Zhao, G.C., Yao, J.L., Wang, W., Xu, Y.J., Wang, Y.J. In Press. Reconstructing South China in Phanerozoic and Precambrian supercontinents. Earth Science Reviews.

Chen, C.H., Liu, Y.H., Lee, C.Y., Xiang, H. and Zhou, H.W., 2012. Geochronology of granulite, charnockite and gneiss in the poly-metamorphosed Gaozhou Complex (Yunkai Massif), South China: Emphasis on the in-situ EMP monazite dating. Lithos, 144(7): 109-129.

Chen, X.Y., Wang, Y.J., Zhang, Y.Z., Zhang, F.F. and Wen, S.N., 2013. Geochemical and Geochronological Characteristics and its Tectonic Sighificance of Andesitic Volcanic Rocks in Chenxing Area, Hainan. Geotectonica et Metallogenia, 37(1): 99-108.

Cocks, L.R.M. and Torsvik, T.H., 2013. The dynamic evolution of the Palaeozoic geography of eastern Asia. Earth-Science Reviews, 117: 40-79.

Compston, W., Williams, I., Kirschvink, J., Zichao, Z. and Guogan, M., 1992. Zircon U-Pb ages for the Early Cambrian time-scale. Journal of the Geological Society, 149(2): 171-184.

Deng, X.G., Chen, Z.Q., Li, X.H. and Liu, D.Y., 2004. Shrimp U-Pb Zircon Dating of the Darongshan-Shiwandashan Granitoid belt in Southeastern Guangxi,China (in Chinese with English Abstract). Geological Review, 50(4): 426-432.

Dickinson, W.R. and Suczek, C.A., 1979. Plate tectonics and sandstone compositions. American Association of Petroleum Geologists Bulletin, 63(12): 2164-2182.

Ding, S., Hu, J., Song, B., Chen, M., Xie, S. and Fan, Y., 2005. U-Pb dating of zircon fromthe bed parallel anatectic granitic intrusion in the Baoban group in Hainan Island and the tectonic implication. Science in China Series D: Earth Sciences, 48(12): 2092-2103.

Ding, S., Xu, C., Long, W., Zhou, Z. and Liao, Z., 2002. Tectonic attribute and geochronology of meta-volcanic rocks, Tunchang, Hainan Island. Acta Geologica Sinica, 18(1): 83-90.

Domeier, M. and Torsvik, T.H., 2014. Plate tectonics in the late Paleozoic. Geoscience Frontiers, 5(3): 303-350.

Du, Y.S., Huang, H., Yang, J.H., Huang, H.W., Tao, P., Huang, Z.Q., Hu, L.S. and Xie, C.X., 2013. The basin translation from Late Paleozoic to Triassic of the Youjiang Basin and its tectonic signification (In Chinese with English abstract). Geological Review, 59(1): 1-11.

Fan, W., Zhang, C., Wang, Y., Guo, F. and Peng, T., 2008. Geochronology and geochemistry of Permian basalts in western Guangxi Province, Southwest China: Evidence for plume-lithosphere interaction. Lithos, 102(1-2): 218-236.

Faure, M., Lepvrier, C., Nguyen, V.V., Vu, V.T., Lin, W. and Chen, Z.C., 2014. The South China block-Indochina collision: Where, When, and how? Journal of Asian Earth Sciences, 79: 260-274.

Faure, M., Lin, W., Chu, Y. and Lepvrier, C., 2016. Triassic tectonics of the southern margin of the South China Block. Comptes Rendus Geoscience, 348(1): 5-14.

Gao, S., Ling, W., Qiu, Y., Lian, Z., Hartmann, G. and Simon, K., 1999. Contrasting geochemical and Sm-Nd isotopic compositions of Archean metasediments from the Kongling high-grade terrain of the Yangtze craton: Evidence for cratonic evolution and redistribution of REE during crustal anatexis. Geochimica et Cosmochimica Acta, 63(13-14): 2071-2088.

Gradstein, F.M., Ogg, J.G., Schmitz, M. and Ogg, G., 2012. The Geologic Time Scale 2012 2-Volume Set, 2. Elsevier.

Greentree, M.R. and Li, Z.X., 2008. The oldest known rocks in south–western China: SHRIMP U–Pb magmatic crystallisation age and detrital provenance analysis of the Paleoproterozoic Dahongshan Group. Journal of Asian Earth Sciences, 33(5): 289-302.

Guo, F., Fan, W.M., Wang, Y.J. and Li, C.W., 2004. Upper Paleozoic basalts in the Southern Yangtze Block: Geochemical and Sr-Nd isotopic evidence for asthenosphere-lithosphere interaction and opening of the Paleo-Tethyan Ocean. International Geology Review, 46(4): 332-346.

Halpin, J.A., Tran, H.T., Lai, C.-K., Meffre, S., Crawford, A.J. and Zaw, K., 2016. U–Pb zircon geochronology and geochemistry from NE Vietnam: A 'tectonically disputed' territory between the Indochina and South China blocks. Gondwana Research, 34: 254-273.

He, B., Xu, Y.-G., Huang, X.-L., Luo, Z.-Y., Shi, Y.-R., Yang, Q.-J. and Yu, S.-Y., 2007. Age and duration of the Emeishan flood volcanism, SW China: geochemistry and SHRIMP zircon U–Pb dating of silicic ignimbrites, post-volcanic Xuanwei Formation and clay tuff at the Chaotian section. Earth and Planetary Science Letters, 255(3): 306-323.

He, H., Wang, Y., Zhang, Y., Chen, X. and Zhou, Y., 2016. Extremely Depleted Carbonferous N-MORB Metabasite at the Chenxing Area(Hainan)and Its Geological Significance (in Chinese with English abstract). Earth Science, 41(8): 1361-1375.

Hu, L., Cawood, P.A., Du, Y., Yang, J. and Jiao, L., 2015a. Late Paleozoic to Early Mesozoic provenance record of Paleo‐Pacific subduction beneath South China. Tectonics, 34(5): 986-1008.

Hu, L., Du, Y., Cawood, P.A., Xu, Y., Yu, W., Zhu, Y. and Yang, J., 2014. Drivers for late Paleozoic to early Mesozoic orogenesis in South China: Constraints from the sedimentary record. Tectonophysics, 618: 107-120.

Hu, L., S., Cawood, P.A., Du, Y.S., Xu, Y.J., Xu, W.C. and Huang, H.W., 2015b. Detrital records for Upper Permian-Lower Triassic succession in the Shiwandashan Basin, South China and implication for Permo-Triassic (Indosinian) orogeny. Journal of Asian Earth Sciences, 98: 152-166.

Hu, L., S., Du, Y.S., Yang, J.H., Huang, H., Huang, H.W. and Huang, H.W., 2012. Geochemistry and Tectonic Significance of Middle Triassic Volcanic Rocks in Nalong, Huangxi Area. Geological Review, 58(3): 481-494.

Huang, H., 2013. The Basin Translation from the Late Paleozoic to Middle Triassic of the Youjiang Basin——Evidence from Geochemistry of Sedimentary and Volcanic Rocks (In Chinese with English Abstract). China University of Geoscience, Wuhan, doctor thesis: 1-160.

Huang, H., Du, Y., Huang, Z., Yang, J., Huang, H., Xie, C. and Hu, L., 2013. Depositional chemistry of chert during late Paleozoic from western Guangxi and its implication for the tectonic evolution of the Youjiang Basin. Science China Earth Sciences: 1-15.

Isozaki, Y., Aoki, K., Nakama, T. and Yanai, S., 2010. New insight into a subduction-related orogen: a reappraisal of the geotectonic framework and evolution of the Japanese Islands. Gondwana Research, 18(1): 82-105.

Isozaki, Y., Aoki, K., Sakata, S. and Hirata, T., 2014. The eastern extension of Paleozoic South China in NE Japan evidenced by detrital zircon. GFF, 136(1): 116-119.

Isozaki, Y., Ehiro, M., Nakahata, H., Aoki, K., Sakata, S. and Hirata, T., 2015. Cambrian plutonism in Northeast Japan and its significance for the earliest arc-trench system of proto-Japan: New U–Pb zircon ages of the oldest granitoids in the Kitakami and Ou Mountains. Journal of Asian Earth Sciences, 108: 136-149.

Jia, X.H., Wang, X.D., Yang, W.Q., Niu, Z.J. and Zhou, D., 2012. LA-ICP-MS zircon U-Pb age of the Nali granite in Qinzhou area of southern Guangxi and its geological significance (in Chnese with English Abstract). Geological Bulletin of China, 31(1): 82-89.

Jian, P., Liu, D., Kröner, A., Zhang, Q., Wang, Y., Sun, X. and Zhang, W., 2009a. Devonian to Permian plate tectonic cycle of the Paleo-Tethys Orogen in southwest China (I): Geochemistry of ophiolites, arc/back-arc assemblages and within-plate igneous rocks. Lithos, 113(3): 748-766.

Jian, P., Liu, D., Kröner, A., Zhang, Q., Wang, Y., Sun, X. and Zhang, W., 2009b. Devonian to Permian plate tectonic cycle of the Paleo-Tethys Orogen in southwest China (II): Insights from zircon ages of ophiolites, arc/back-arc assemblages and within-plate igneous rocks and generation of the Emeishan CFB province. Lithos, 113(3): 767-784.

Jian, P., Liu, D. and Sun, X., 2003. SHRIMP Dating of Baimaxueshan and Ludian Granitoid Batholiths, Northwestern Yunnan Province, and Its Geological Implicatins. Acta Geoscientia Sinica, 24(4; ISSU 77): 337-342.

Lai, C.-K., Meffre, S., Crawford, A.J., Zaw, K., Xue, C.-D. and Halpin, J.A., 2014. The Western Ailaoshan Volcanic Belts and their SE Asia connection: a new tectonic model for the Eastern Indochina Block. Gondwana Research, 26(1): 52-74.

Lehrmann, D.J., Chaikin, D.H., Enos, P., Minzoni, M., Payne, J.L., Yu, M., Goers, A., Wood, T., Richter, P. and Kelley, B.M., 2014. Patterns of basin fill in Triassic turbidites of the Nanpanjiang basin: implications for regional tectonics and impacts on carbonate‐platform evolution. Basin Research, 27: 587-612.

Lehrmann, D.J., Donghong, P., Enos, P., Minzoni, M., Ellwood, B.B., Orchard, M.J., Jiyan, Z., Jiayong, W., Dillett, P. and Koenig, J., 2007a. Impact of differential tectonic subsidence on isolated carbonate-platform evolution: Triassic of the Nanpanjiang Basin, south China. AAPG bulletin, 91(3): 287-320.

Lehrmann, D.J., Payne, J.L., Pei, D., Enos, P., Druke, D., Steffen, K., Zhang, J., Wei, J., Orchard, M.J. and Ellwood, B., 2007b. Record of the end-Permian extinction and Triassic biotic recovery in the Chongzuo-Pingguo platform, southern Nanpanjiang basin, Guangxi, south China. Palaeogeography, Palaeoclimatology, Palaeoecology, 252(1): 200-217.

Lepvrier, C., Faure, M., Van, V.N., Van Vu, T., Lin, W., Trong, T.T. and Hoa, P.T., 2011. North-directed Triassic nappes in Northeastern Vietnam (East Bac Bo). Journal of Asian Earth Sciences, 41: 56-68.

Lepvrier, C., Maluski, H., Van Tich, V., Leyreloup, A., Truong Thi, P. and Van Vuong, N., 2004. The early Triassic Indosinian orogeny in Vietnam (Truong Son Belt and Kontum Massif); implications for the geodynamic evolution of Indochina. Tectonophysics, 393(1-4): 87-118.

Lepvrier, C., Van Vuong, N., Maluski, H., Truong Thi, P. and Van Vu, T., 2008. Indosinian tectonics in

Vietnam. Comptes Rendus Geosciences, 340(2-3): 94-111.

Li, J.H., Zhao, G.C., Johnston, S.T, Dong, S.W., Zhang, Y.Q., Xin Y.J., Wang, W.B., Sun, H.S., Yu, Y.G. In press. Permo-Triassic structural evolution of the Shiwandashan and Youjiang structural belts, South China. Journal of Structural Geology, DOI: 10.1016/j.jsg.2017.05.004

Li, X.H., Li, W.X., Li, Z.X. and Liu, Y., 2008. 850-790 Ma bimodal volcanic and intrusive rocks in northern Zhejiang, South China: A major episode of continental rift magmatism during the breakup of Rodinia. Lithos, 102(1-2): 341-357.

Li, X.H., Li, Z.X., He, B., Li, W.X., Li, Q.L., Gao, Y.Y. and Wang, X.C., 2012. The Early Permian active continental margin and crustal growth of the Cathaysia Block: In situ U-Pb, Lu-Hf and O isotope analyses of detrital zircons. Chemical geology, 328: 195-207.

Li, X.H., Li, Z.X., Li, W.X. and Wang, Y., 2006. Initiation of the Indosinian orogeny in South China: Evidence for a Permian magmatic arc on Hainan Island. The Journal of geology, 114(3): 341-353.

Li, Z.X., Li, X., Zhou, H. and Kinny, P.D., 2002. Grenvillian continental collision in south China: New SHRIMP U-Pb zircon results and implications for the configuration of Rodinia. Geology, 30(2): 163-166.

Li, Z.X. and Li, X.H., 2007. Formation of the 1300-km-wide intracontinental orogen and postorogenic magmatic province in Mesozoic South China: A flat-slab subduction model. Geology, 35(2): 179-182.

Li, Z.X., Wartho, J.A., Occhipinti, S., Zhang, C.L., Li, X.H., Wang, J. and Bao, C., 2007. Early history of the eastern Sibao Orogen (South China) during the assembly of Rodinia: New mica 40Ar/39Ar dating and SHRIMP U-Pb detrital zircon provenance constraints. Precambrian Research, 159(1-2): 79-94.

Liang, X. and Li, X., 2005. Late Permian to Middle Triassic sedimentary records in Shiwandashan Basin: Implication for the Indosinian Yunkai Orogenic Belt, South China. Sedimentary Geology, 177(3-4): 297-320.

Liang, X.Q., Zhou, Y., Jiang, Y., Wen, S.N., Fu, J.G. and Wang, C., 2013. Different of sedimentary response to Dongwu Movement: Study on LA-ICPMS U-Pb ages of detrital zircons from Upper Permian Wujiaping or Longtan Formation from the Yangtze and Cathaysia blocks. Acta Petrologica Sinica, 29(10): 3592-3602.

Liu, C., Deng, J. and Shi, Y.L., 2011. Characteristics of volcanic rocks from Late Permian to Early Triassic in Ailaoshan tectono-magmatic belt and implications for tectonic settings (in Chinese with English abstract). Acta Petrologica Sinica, 27(12): 3590-3602.

Liu, J., Tran, M.-D., Tang, Y., Nguyen, Q.-L., Tran, T.-H., Wu, W., Chen, J., Zhang, Z. and Zhao, Z., 2012. Permo-Triassic granitoids in the northern part of the Truong Son belt, NW Vietnam: Geochronology, geochemistry and tectonic implications. Gondwana Research, 22(2): 628-644.

Liu, Y., Gao, S., Hu, Z., Gao, C., Zong, K. and Wang, D., 2010. Continental and oceanic crust recycling-induced melt–peridotite interactions in the Trans-North China Orogen: U–Pb dating, Hf isotopes and trace elements in zircons from mantle xenoliths. Journal of Petrology, 51(1-2): 537-571.

Long, W.G., Tong, J.N., Zhu, Y.H., Zhou, J.B., Li, S.X., Shi, C. 2007. Discovery of the Permian in the Danzhou-Tunchang area of Hainan Island and its geological significance (in Chinese with English abstract). Geology and Mineral Resources of South China, 01: 0038-0045

Luding, K.R., 2003. Isoplot 3.00, a Geochronological Toolkit for Microsoft Excel. Berkeley Geochronology Center. Special Publication, 4: 1-70.

McLennan, S., Hemming, S., McDaniel, D. and Hanson, G., 1993. Geochemical approaches to sedimentation, provenance, and tectonics. Speical Papers-Geological Society America: 21-21.

Meng, Y.Y., Zhou, Q.E. and Yu-Kun, L.I., 2002. The characteristics and controlling sedimentary facies and granitold analysis of the middle part of Pingxiang-Dongmen large fault-An example of Ningming-Banxi Regions. Guangxi Geology, 15(4): 1-5.

Metcalfe, I., 2006. Palaeozoic and Mesozoic tectonic evolution and palaeogeography of East Asian crustal fragments: The Korean Peninsula in context. Gondwana Research, 9(1–2): 24-46.

Metcalfe, I., 2011. Palaeozoic–Mesozoic history of SE Asia. Geological Society, London, Special Publications, 355(1): 7-35.

Mou, C.L. and Wang, L.Q., 2000. The Evolution of the Volcano-sedimentary Basin During the Late Triassic in Deqia, Yunnan (in Chinese with English abstract). J mineral Petrol, 20(3): 23-28.

Nie, X., Feng, Q., Metcalfe, I., Baxter, A.T. and Liu, G., 2016. Discovery of a Late Devonian magmatic arc in the southern Lancangjiang zone, western Yunnan: Geochemical and zircon U–Pb geochronological constraints on the evolution of Tethyan ocean basins in SW China. Journal of Asian Earth Sciences, 118: 32-50.

Peng, S., Jin, Z., Liu, Y., Fu, J., He, L., Cai, M. and Wang, Y., 2006. Petrochemistry, chronology and tectonic setting of strong peraluminous anatectic granitoids in Yunkai Orogenic Belt, western Guangdong Province, China. Journal of China University of Geosciences, 17(1): 1-12.

Qin, X., Wang, Z., Zhang, Y., Pan, L., Guiang, H.U. and Zhou, F., 2012. Geochemistry of Permian Mafic Igneous Rocks from the Napo-Qinzhou Tectonic Belt in Southwest Guangxi, Southwest China: Implications for Arc-Back Arc Basin Magmatic Evolution. Acta Geologica Sinica (English Edition), 86(5): 1182-1199.

Qin, X.F., Wang, Z.C., Zhang, Y.L., Pan, L.Z., Hu, G.A. and Zhou, F.S., 2011. Geochronology and geochemistry of Early Mesozoic acid volvanic rocks from Southwest Guangxi: Constraints on tectonic evolution of the southwestern segment of Qinzhou-Hangzhou joiny belt (In Chinese with English abstract). Acta Petrologica Sinica, 27(3): 794-808.

Qiu, L., Yan, D.-P., Yang, W.-X., Wang, J., Tang, X. and Ariser, S., In Press. Early to Middle Triassic sedimentary records in the Youjiang Basin, South China: Implications for Indosinian orogenesis. Journal of Asian Earth Sciences.

Reid, A., Wilson, C.J., Shun, L., Pearson, N. and Belousova, E., 2007. Mesozoic plutons of the Yidun Arc, SW China: U/Pb geochronology and Hf isotopic signature. Ore Geology Reviews, 31(1): 88-106.

Roger, F., Maluski, H., Lepvrier, C., Vu Van, T. and Paquette, J.-L., 2012. LA-ICPMS zircons U/Pb dating of Permo-Triassic and Cretaceous magmatisms in Northern Vietnam–Geodynamical implications. Journal of Asian Earth Sciences, 48: 72-82.

Searle, M.P., Yeh, M.-W., Lin, T.-H. and Chung, S.-L., 2010. Structural constraints on the timing of left-lateral shear along the Red River shear zone in the Ailao Shan and Diancang Shan Ranges, Yunnan, SW China. Geosphere, 6(4): 316-338.

Song, B., Yan, Q.R., Xiang, Z.J., Chen, H.M., Ma, T.Q. and Yang, G.Y., 2013. Sedimentary Characteristics and Tectonic Setting of the Middle Triassic Pingxiang Basin, Guangxi (in Chinese with English Abstract). Acta Geologica Sinica, 87(4): 453-473.

Sun, S.S. and McDonough, W., 1989. Chemical and isotopic systematics of oceanic basalts: implications

for mantle composition and processes. Geological Society, London, Special Publications, 42(1): 313-345.

Tan, F.W., 2002. The Sedimentary Characteristics of Simao Triassic Rear Arc Foreland Basin, Yunnan Province (in Chinese with English abstract). Acta Sedimentological Sinica, 20(4): 0560-0567.

Tang, Z.Y., Feng, S.N., 1998. Discovery of the Permian system in the Daling area of Hainan Island and its significance (in Chinese with English abstract). Journal of Stratigraphy, 22(3): 232-240.

Taylor, S.R. and McLennan, S.M., 1985. The continental crust: its composition and evolution. Blackwell, oxford: pp. 1-312.

Thanh, N.X., Hai, T.T., Hoang, N., Lan, V.Q., Kwon, S., Itaya, T. and Santosh, M., 2014. Backarc mafic–ultramafic magmatism in Northeastern Vietnam and its regional tectonic significance. Journal of Asian Earth Sciences, 90: 45-60.

Tran, V.T. and Khuc., V., 2011. Geology and natural resources of Vietnam. Natural Sciences and Technology Publishing House, Hanoi.

V Vượng, N., Hansen, B.T., Wemmer, K., Lepvrier, C., V Tích, V. and Trọng Thắng, T., 2013. U/Pb and Sm/Nd dating on ophiolitic rocks of the Song Ma suture zone (northern Vietnam): evidence for upper paleozoic paleotethyan lithospheric remnants. Journal of Geodynamics, 69: 140-147.

Wang, B.-d., Wang, L.-q., Wang, D.-b. and Zhang, W.-p., 2011a. Zircon U-Pb dating of volcanic rocks from Renzhixueshan Formation in Shangdie rift basin of Sanjiang area and its geological implications (In Chinese with English Abstract). Acta Petrologica Et Mineralogica, 30: 25-33.

Wang, H. and Mo, X., 1995. An outline of the tectonic evolution of China. Episodes, 18: 6-6.

Wang, L.J., Yu, J.H., Griffin, W. and O'Reilly, S., 2011b. Early crustal evolution in the western Yangtze Block: Evidence from U-Pb and Lu-Hf isotopes on detrital zircons from sedimentary rocks. Precambrian Research, 222: 368-385.

Wang, L.Q., Pan, G.T., Li, D.M., Xu, Q. and Lin, S.L., 1999. The Spatio-temporal Framework Geological Evolution of the Jinshajiang Arc-Basin Systems (in Chinese with English abstract). Acta Geologica Sinica, 73(3): 206-218.

Wang, Y., Fan, W., Zhang, G. and Zhang, Y., 2013a. Phanerozoic tectonics of the South China Block: key observations and controversies. Gondwana Research, 23(4): 1273-1305.

Wang, Y., Fan, W., Zhao, G., Ji, S. and Peng, T., 2007. Zircon U-Pb geochronology of gneissic rocks in the Yunkai massif and its implications on the Caledonian event in the South China Block. Gondwana Research, 12(4): 404-416.

Wang, Y., Wu, C., Zhang, A., Fan, W., Zhang, Y., Peng, T. and Yin, C., 2012. Kwangsian and Indosinian reworking of the eastern South China Block: Constraints on zircon U-Pb geochronology and metamorphism of amphibolites and granulites. Lithos, 150: 227-242.

Wang, Y., Zhang, A., Cawood, P.A., Fan, W., Xu, J., Zhang, G. and Zhang, Y., 2013b. Geochronological, geochemical and Nd-Hf-Os isotopic fingerprinting of an early Neoproterozoic arc-back-arc system in South China and its accretionary assembly along the margin of Rodinia. Precambrian Research, 231: 343-371.

Wang, Y., Zhang, A., Fan, W., Zhao, G., Zhang, G., Zhang, Y., Zhang, F. and Li, S., 2011c. Kwangsian crustal anatexis within the eastern South China Block: Geochemical, zircon U-Pb geochronological and Hf isotopic fingerprints from the gneissoid granites of Wugong and Wuyi-Yunkai Domains. Lithos, 127: 239-260.

Wang, Y., Zhang, F., Fan, W., Zhang, G., Chen, S., Cawood, P.A. and Zhang, A., 2010. Tectonic setting of

the South China Block in the early Paleozoic: Resolving intracontinental and ocean closure models from detrital zircon U-Pb geochronology. Tectonics, 29(6): TC6020.

Wang, Z.L., Xu, D.R., Wu, C.J., Fu, W.W., Wang, L. and Wu, J., 2013c. Discovery of the Late Paleozoic ocean island basalts (OIB) in Hainan Island and their geodynamic implications. Acta Petrologica Sinica, 029(03): 0875-0886.

Wu, G., Zhong, D., Zhang, Q. and Ji, J., 1999. Babu - Phu Ngu Ophiolites: A Geological Record of Paleotethyan Ocean Bordering China and Vietnam. Gondwana Research, 2(4): 554-557.

Wu, G.Y., Ji, J.Q., He, S.D. and Zhong, D.L., 2002. Early Permian Magmatic Arc in Pingxiang, Guangxi and its Tecotonic Implications (in Chinese with English Abstract). J. Minenral Petrol, 22(3): 61-65.

Xia, Y., Xu, X.-S. and Zhu, K.-Y., 2012. Paleoproterozoic S-and A-type granites in southwestern Zhejiang: Magmatism, metamorphism and implications for the crustal evolution of the Cathaysia basement. Precambrian Research, 216: 177-207.

Xiao, L., Xu, Y.-G., Chung, S.-L., He, B. and Mei, H., 2003. Chemostratigraphic correlation of Upper Permian lavas from Yunnan Province, China: extent of the Emeishan large igneous province. International Geology Review, 45(8): 753-766.

Xie, C., Zhu, J., Ding, S., Zhang, Y., Fu, T. and Li, Z., 2006a. Identification of Hercynian shoshonitic intrusive rocks in central Hainan Island and its geotectonic implications. Chinese Science Bulletin, 51(20): 2507-2519.

Xie, J., Chang, X.Y. and Zhu, B.Q., 2006b. Geochemical characteristics of Permian volcanic rocks from jianshui, southeast Yunnan and their tectonic imlication (in Chinese with English Abstract). Journal of the Graduate School of the China Academy of Sciences, 23(3): 349-356.

Xu, Y., Cawood, P.A., Du, Y., Huang, H. and Wang, X., 2014a. Early Paleozoic orogenesis along Gondwana's northern margin constrained by provenance data from South China. Tectonophysics, 636: 40-51.

Xu, Y., Cawood, P.A., Du, Y., Zhong, Z. and Hughes, N.C., 2014b. Terminal suturing of Gondwana along the southern margin of South China Craton: Evidence from detrital zircon U‐Pb ages and Hf isotopes in Cambrian and Ordovician strata, Hainan Island. Tectonics, 33(12): 2490-2504.

Xu, Y.J., Cawood, P.A., Du, Y.S. and Hu, L., S., In Press. An Aulacogen responding to opening of the Ailaoshan Ocean: Origin of the Qin-Fang Trough in South China. Journal of Geology.

Yang, J., Cawood, P.A., Du, Y., Huang, H. and Hu, L., 2012a. Detrital record of Indosinian mountain building in SW China: Provenance of the Middle Triassic turbidites in the Youjiang Basin. Tectonophysics, 574-575: 105-117.

Yang, J., Cawood, P.A., Du, Y., Huang, H. and Hu, L., 2013. A sedimentary archive of tectonic switching from Emeishan Plume to Indosinian orogenic sources in SW China. Journal of the Geological Society: 2012-143.

Yang, J., Cawood, P.A., Du, Y., Huang, H. and Tao, P., 2012b. Large Igneous Province and magmatic arc sourced Permian-Triassic volcanogenic sediments in China. Sedimentary Geology, 261-262: 120-131.

Yao, W., Li, Z.X., Li, W.X. and Li, X.H., 2017. Proterozoic tectonics of Hainan Island in supercontinent cycles: new insights from geochronological and isotopic results. Precambrian Research, 290: 86-100.

Yin, C., Lin, S., Davis, D.W., Xing, G., Davis, W.J., Cheng, G., Xiao, W. and Li, L., 2013. Tectonic evolution of the southeastern margin of the Yangtze Block: Constraints from SHRIMP U-Pb and LA-ICP-MS Hf isotopic studies of zircon from the eastern Jiangnan Orogenic Belt and

implications for the tectonic interpretation of South China. Precambrian Research, 236: 145-156.

Yu, J.H., O'Reilly, S.Y., Wang, L., Griffin, W.L., Zhou, M.F., Zhang, M. and Shu, L., 2010. Components and episodic growth of Precambrian crust in the Cathaysia Block, South China: Evidence from U-Pb ages and Hf isotopes of zircons in Neoproterozoic sediments. Precambrian Research, 181(1-4): 97-114.

Yu, J.H., Wang, L., O'Reilly, S., Griffin, W., Zhang, M., Li, C. and Shu, L., 2009. A Paleoproterozoic orogeny recorded in a long-lived cratonic remnant (Wuyishan terrane), eastern Cathaysia Block, China. Precambrian Research, 174(3-4): 347-363.

Yuan, H., Gao, S., Liu, X., Li, H., Günther, D. and Wu, F., 2004. Accurate U‐Pb age and trace element determinations of zircon by laser ablation‐inductively coupled plasma‐mass spectrometry. Geostandards and Geoanalytical Research, 28(3): 353-370.

Zeng, Y., Liu, W., Cheng, H., Zheng, R., Zhang, J., Li, X. and Jiang, T., 1995. Evolution of Sedimentation and Tectonics of the Youjiang Composite Basin, South China. Acta Geologica Sinica (English Edition), 8(4): 358-371.

Zhang, F., Wang, Y., Chen, X., Fan, W., Zhang, Y., Zhang, G. and Zhang, A., 2011a. Triassic high-strain shear zones in Hainan Island (South China) and their implications on the amalgamation of the Indochina and South China Blocks: Kinematic and 40Ar/39Ar geochronological constraints. Gondwana Research, 19: 439-460.

Zhang, K.J. and Cai, J.X., 2009. NE–SW-trending Hepu–Hetai dextral shear zone in southern China: Penetration of the Yunkai Promontory of South China into Indochina. Journal of Structural Geology, 31(7): 737-748.

Zhang, R., LO, C.H., CHUNG, S.L., Grove, M., Omori, S., Iizuka, Y., Liou, J. and Tri, T., 2013. Origin and tectonic implication of ophiolite and eclogite in the Song Ma suture zone between the South China and Indochina blocks. Journal of Metamorphic Geology, 31(1): 49-62.

Zhang, W.P., Wang, L.Q., Wang, B.D., Wang, D.B., Dai, J. and Liu, W., 2011b. Chronology, geochemistry and petrogenesis of Deqin granodiorite body in the middle section of Jiangda-Weixi arc (in chinese with English abstract). Acta Petrologica Sinica, 27: 2577-2590.

Zhao, G. and Cawood, P.A., 2012. Precambrian geology of China. Precambrian Research, 222-223: 13-54.

Zhao, L., Guo, F., Fan, W., Li, C., Qin, X. and Li, H., 2012. Origin of the granulite enclaves in Indo-Sinian peraluminous granites, South China and its implication for crustal anatexis. Lithos, 150: 209-226.

Zhao, L., Guo, F., Fan, W.M., Li, C.W., Qin, X.F. and Li, H.X., 2010. Crustal evolution of the Shiwandashan area in South China: Zircon U-Pb-Hf isotopic records from granulite enclaves in Indo-Sinian granites. Chinese Science Bulletin, 55(19): 2028-2038.

Zhong, D.L., Wu, G.Y., Ji, J.Q., Zhang, Q. and Ding, L., 1998. Discovery of the ophiolites in southeastern Yunnan, China (In Chinese). Chinese Science Bulletin, 43: 1365-1369.

Zhou, Y., Liang, X., Liang, X., Jiang, Y., Wang, C., Fu, J. and Shao, T., 2015. U–Pb geochronology and Hf-isotopes on detrital zircons of Lower Paleozoic strata from Hainan Island: New clues for the early crustal evolution of southeastern South China. Gondwana Research, 27(4): 1586-1598.

Zhu, J.-J., Hu, R.-Z., Bi, X.-W., Zhong, H. and Chen, H., 2011. Zircon U–Pb ages, Hf–O isotopes and whole-rock Sr–Nd–Pb isotopic geochemistry of granitoids in the Jinshajiang suture zone, SW

China: Constraints on petrogenesis and tectonic evolution of the Paleo-Tethys Ocean. Lithos, 126(3): 248-264.

Zi, J.W., Cawood, P.A., Fan, W.M., Tohver, E., Wang, Y.J., McCuaig, T.C. and Peng, T.P., 2013. Late Permian-Triassic magmatic evolution in the Jinshajiang orogenic belt, SW China and implications for orogenic processes following closure of the Paleo-Tethys. American Journal of Science, 313(2): 81-112.

Zi, J.W., Cawood, P.A., Fan, W.M., Wang, Y.J. and Tohver, E., 2012a. Contrasting rift and subduction‐related plagiogranites in the Jinshajiang ophiolitic mélange, southwest China, and implications for the Paleo‐Tethys. Tectonics, 31: TC2012, doi:10.1029/2011TC002937, 2012.

Zi, J.W., Cawood, P.A., Fan, W.M., Wang, Y.J., Tohver, E., McCuaig, T.C. and Peng, T.P., 2012b. Triassic collision in the Paleo-Tethys Ocean constrained by volcanic activity in SW China. Lithos, 144-145: 145-160.

Figure Captions

Fig. 1. A: Tectonic framework of the East Asia (revised from Metcalfe (2006).

B: simplified geological map of the South China Block and location of the

study areas (base on the 1:5000000 geology map of China).

Fig. 2. A and B: Geological map of the Pingxiang-Chongzuo area and location of measured sections (modified from 1:250000 Geologic Map of the Pingxiang area); C: Geological map of the Hainan Island and location of analyzed samples (modified from 1:1000000 Geologic Map of Hainan Island). Abbreviations: C_2-P, Late

Carboniferous-Permian; C, Carboniferous ; P, Permian; T_1n, Lower Triassic Nanhong Formation; T_1l, Lower Triassic Luolou Formation; $T_{1-2}b$, Lower-Middle Triassic Besi Formation; T_2b, Middle Triassic Banna Formation; T_2l, Middle Triassic Lanmu Formation; J-Q, Jurassic-Quaternary

Fig. 3. Measured sections through the Lower-Middle Triassic succession in the Pingxiang-Chongzuo area and showing stratigraphic position of analyzed samples. Abbreviations: LP, Late Permian; ET, Early Triassic; MT, Middle Triassic.

Fig. 4. Representative field photographs of Permian and Lower-Middle Triassic sequence in Hainan Island and Pingxiang-Chongzuo area; A, B) gray siltstone-mudstone of the Lower Triassic Nanhong Formation at Zaimiao section; C) thick sandstone interlay with thin mudstone-siltstone, Zaimiao section; D, E, F) parallel and cross-bedding within Lower Triassic Nanhong Formation, Zaimiao section; G) parallel bedding within the Middle Triassic Banna Formation, Anzhen, Pingxiang area; H) thick sandstone interbedded with thin mudstone of Middle Triassic Banna Formation; I) wave bedding within Middle Triassic Banna Formation siltstone, Kengying, Pingxiang area; J) mudstone and limestone contact in the low part of the Banna Formation, Anzhen, Pingxiang area; K) limestone conglomerate in the low part of the Banna Formation, Anzhen, Pingxiang area; L) Permian siltstone in the Danzhou, Hainan Island, M) thin mudstone of the Middle Triassic Lanmu Formation, Ping'er, Pingxiang; N, O) parallel and cross beddings within Middle Triassic Banna and Lanmu Formation, Pingxiang area, P) Permian siltstone in the Jiangbian area, Hainan Island.

Fig. 5. Photomicrographs of Permian and Lower-Middle Triassic sequence in Hainan Island and Pingxiang-Chongzuo area, A, B) sandstone of Lower Triassic Nanhong Formation in Pingxiang-Chongzuo area; C) sandstone of Middle Triassic Banna Formation in Pingxiang-Chongzuo area; D, E) sandstone of Middle Triassic Lanmu Formation in Pingxiang-Chongzuo area and (F) siltstone of Permian on Hainan island.

Fig. 6. QFL, QmFLt and QpLvLs diagrams for the Triassic samples of Pingxiang-Chongzuo area (after Dickinson and Suczek (1979). Q, total quartz; F, total feldspar; L, lithic fragment; Qm, monocrystalline quartz; Qp, polycrystalline quartz; Lv, volcanic lithic fragment; Ls, sedimentary lithic fragment; Lt=L+Qp.

Fig. 7. Primitive-normalized REE patterns (A), spider diagrams (B), Th versus Th/U (C) Zr/Sc versus Th/Sc (D), Th-Sc-Zr/10 and La-Th-Sc diagrams for the Triassic samples of Pingxiang-Chongzuo area, (E) Th-Sc-Zr/10 and La-Th-Sc diagrams modified after Bhatia and Crook (1986) and Permo-Triassic data from Yang et al., 2012a; Hu et al., 2014 and this study. Chondrite data and primitive mantle data are from Sun and McDonough (1989); Th/Sc-Zr/Sc diagram after Mclennan et al. (1993), Average upper continental crust (Taylor and McLennan, 1985) is plotted on diagrams for comparision;

Fig. 8. Relative probability plots and age histograms of detrital zircons of samples in Permian on Hainan Island and Lower-Middle Triassic sequence of Pingxiang-Chongzuo area

Fig. 9. Schematic time-space diagram for the southern margin of South China Craton. Abbreviations; Roadi-Roadian; Wordi-Wordian; Capit-Capitanian;

Wuch-Wuchiapingian; Chang-Changhsingian; Indu-Induan; Olene-Olenekian; Anisi-Anisian; Ladin-Ladinian; Carni-Carnian; Noria-Norian; Rhae-Rhaetian. The numerical and stage time scales are those of Gradstein and others (2012). Paleo-Tethys subduction is from Zi et al.(2013) and the Emeishan Large Igneous event is from Xiao et al. (2003), He et al. (2007) and Fan et al. (2008). Lithotectonic units, timing of tectonothermal events and basins sources: Jinshajiang-Ailaoshan Ocean Basin (BGMRYP, 1990; Wang et al., 1999; Mou and Wang, 2000; Tan, 2002; Jian et al., 2003; Reid et al., 2007; Jian et al., 2009a; Searle et al., 2010; Liu et al., 2011; Wang et al., 2011a; Zhang et al., 2011b; Zhu et al., 2011; Zi et al., 2012a; Zi et al., 2012b; Zi et al., 2013; Nie et al., 2016); Youjiang area of Greater Youjiang Basin (BGMRGR, 1985; Fan et al., 2008; Hu et al., 2012; Yang et al., 2012a; Yang et al., 2012b; Du et al., 2013; Huang, 2013; Qiu et al., In Press); Pingxiang-Chongzuo area of Greater Youjiang Basin (BGMRGR, 1985; Qin et al., 2012; Song et al., 2013 and our unpublished data); Qinfang area of Greater Youjiang Basin (BGMRGR, 1985; Deng et al., 2004; Liang and Li, 2005; Zhao et al., 2010; Wang et al., 2012; Hu et al., 2014; Hu et al., 2015b); Hainan Island (BGMRGP, 1988; Ding et al., 2005; Xie et al., 2006a; Xie et al., 2006b; Li and Li, 2007; Zhang et al., 2011a; Wang et al., 2012; Chen et al., 2013; He et al., 2016); North Vietnam (Tran and Khuc., 2011; Roger et al., 2012; Thanh et al., 2014; Halpin et al., 2016), Song Ma zone (Lepvrier et al., 2004; Lepvrier et al., 2011; Liu et al., 2012; V Vượng et al., 2013; Faure et al., 2014; Lai et al., 2014)

Fig. 10. Probability density diagram comparing detrital zircons age patterns in

Permo-Triassic succession of South China Craton and North Vietnam

Fig. 11. Probability density diagram comparing Phanerozoic detrital zircons models in Permo-Triassic succession of South China Craton and North Vietnam

Fig. 12. Cumulative probability curves of measured crystallization age for a detrital zircon grains relative to the depositional age of Permo-Triassic samples in Greater Youjiang Basin and Hainan Island (modified from Cawood et al. (2012)), data from Yang et al., 2012a, Hu et al., 2014, 2015a and this study, convergent basin (A, rose red), collisional basin (B, blue), and extensional basin (C, green), transition between convergent-collisional setting (purple), convergent-extensional setting (brown), and collisional-extensional setting (blue-green and brown).

Fig. 13. Model for schematic paleogeographic evolution of the Greater Youjiang Basin in Permo-Triassic, showing derivation of detritus in the Greater Youjiang Basin from inner craton and syn-orogenic belts in the south-southwest of the basin, based on Yang et al. (2012a), Lehrmann et al., (2014), Hu et al. (2015b), Du et al. (2013). Zi et al. (2013), Faure et al. (2014) and this study. Abbreviation: SCC - South China Craton; JA zone - Jingshajiang-Ailaoshan suture zone; S (B) zone - Song Ma (Babu) suture zone; PC/PC area - Pingxiang-Chongzuo area; HN - Hainan Island, the Yong'an Basin located in east of the Greater Youjiang Basin and unmarked in this diagram.

Fig. 14. Paleogeograhpy reconstruction diagrams of South China Craton in Permo-Triassic (modified after Li and Li (2007); Cocks and Torsvik (2013) and Domeier and Torsvik (2014))

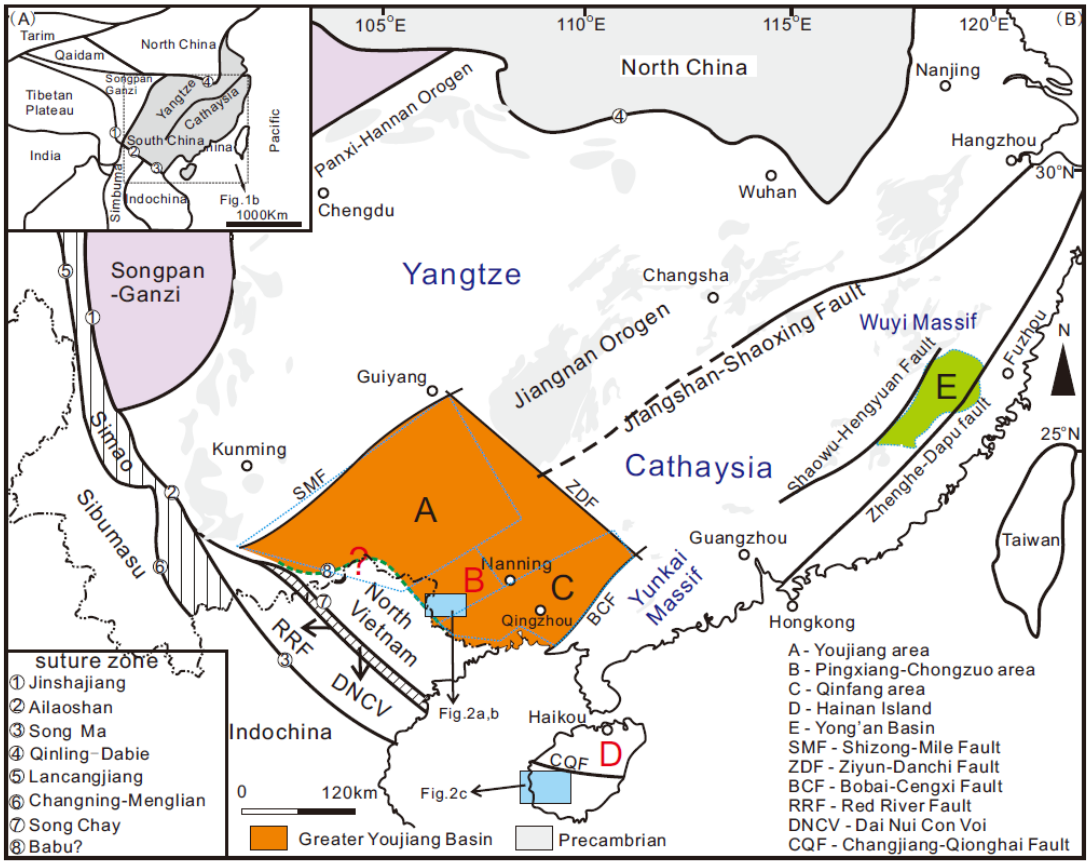

Figure 1

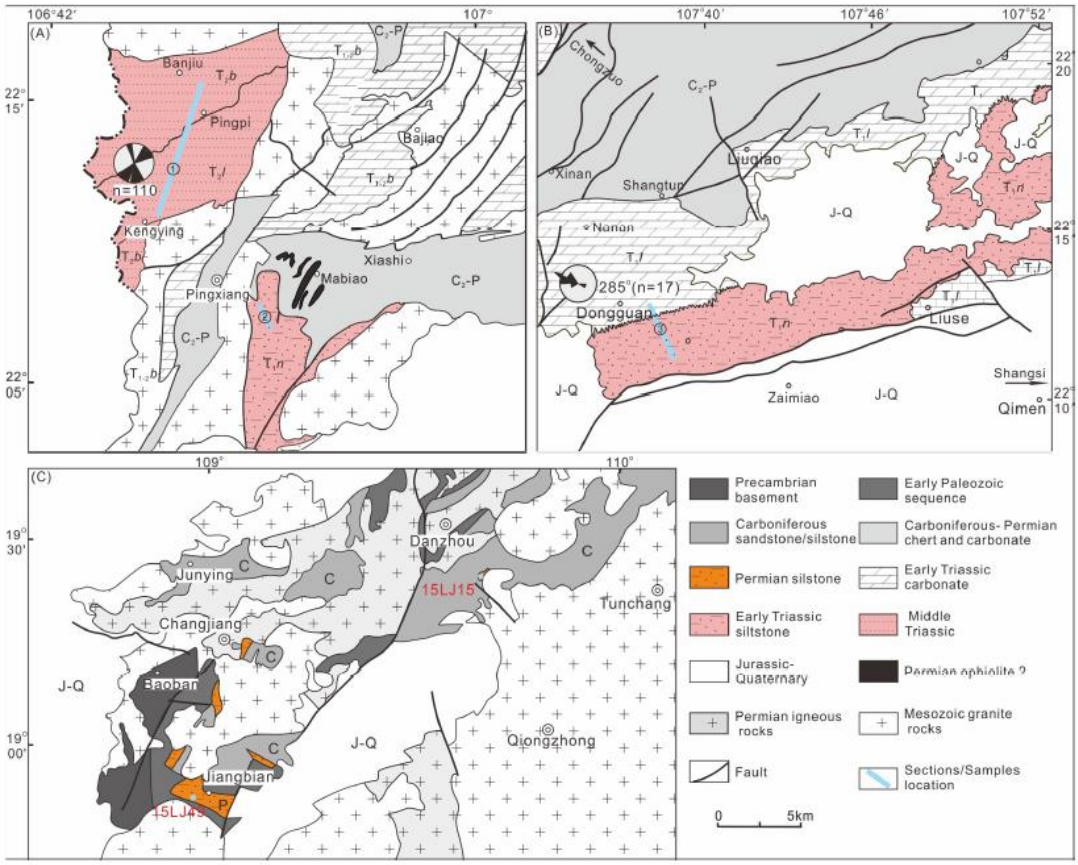

Figure 2

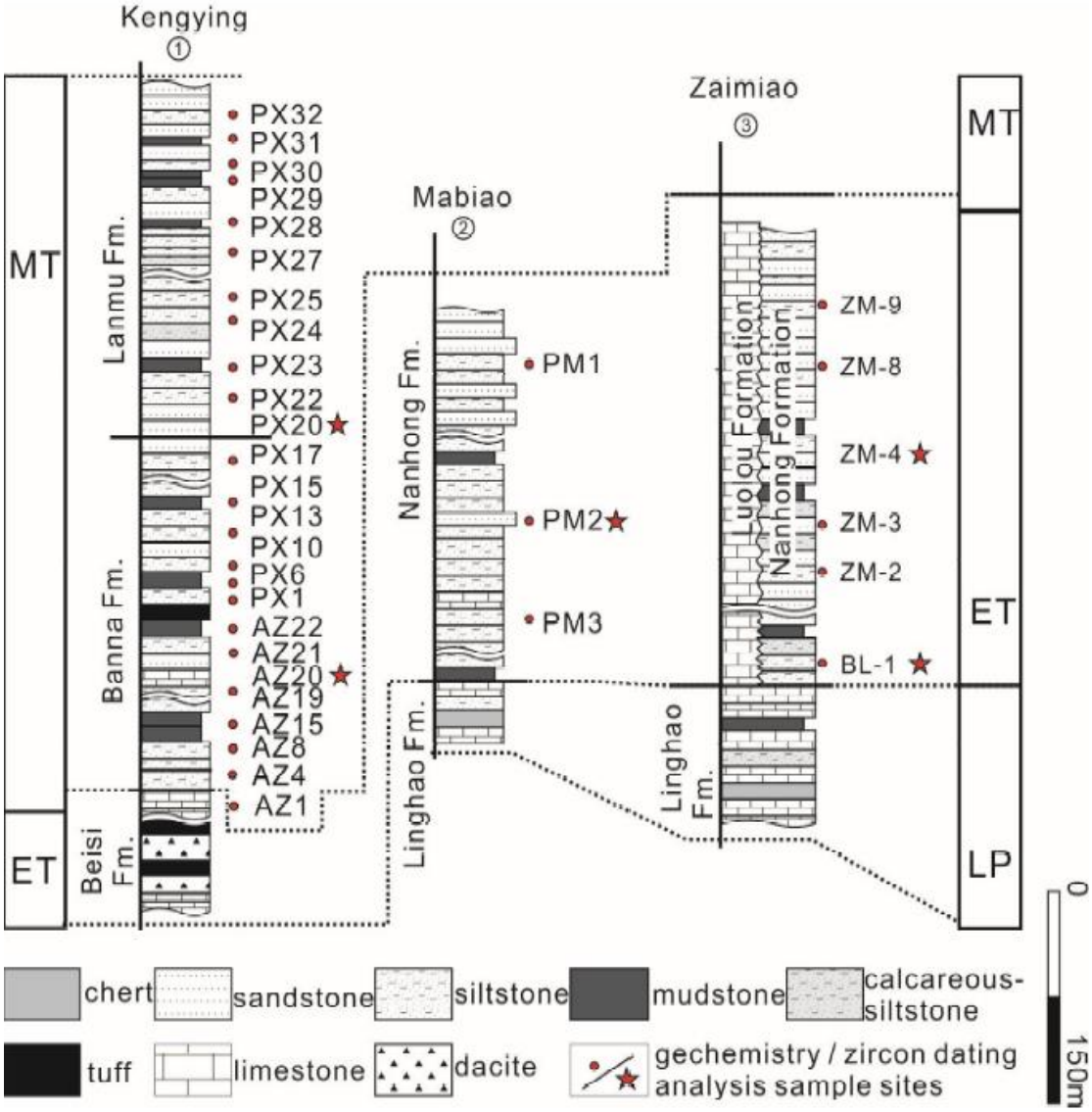

Figure 3

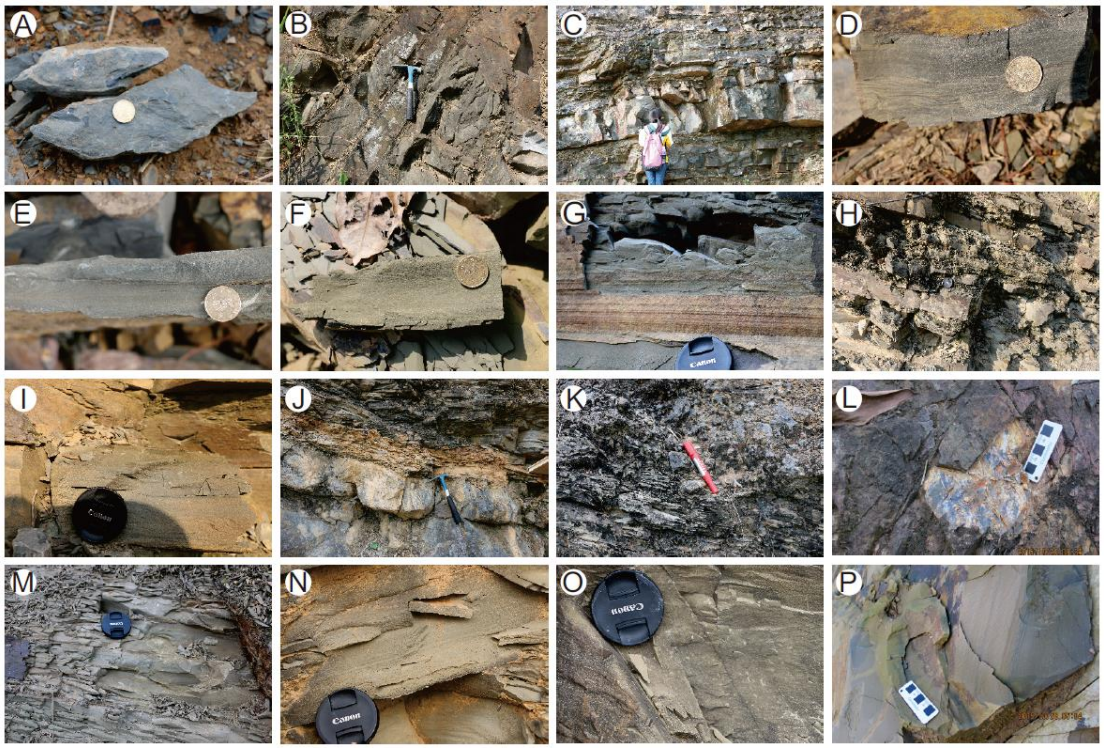

Figure 4

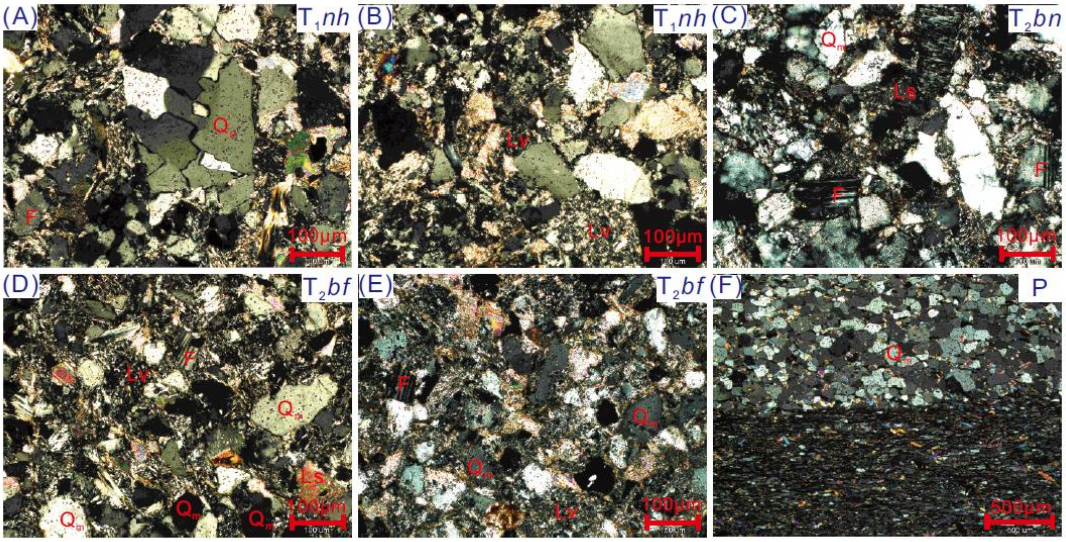

Figure 5

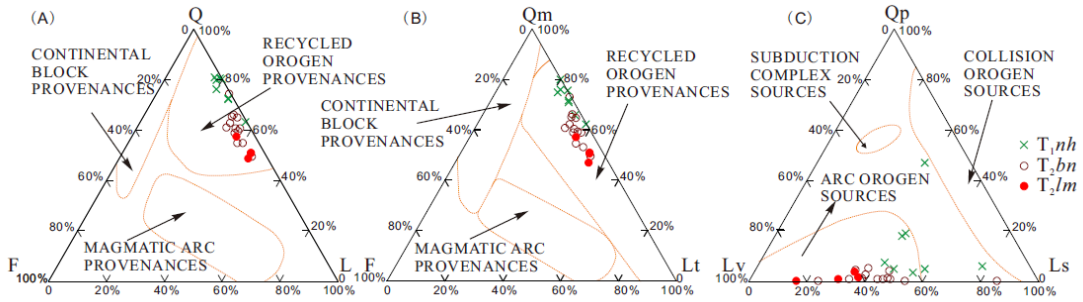

Figure 6

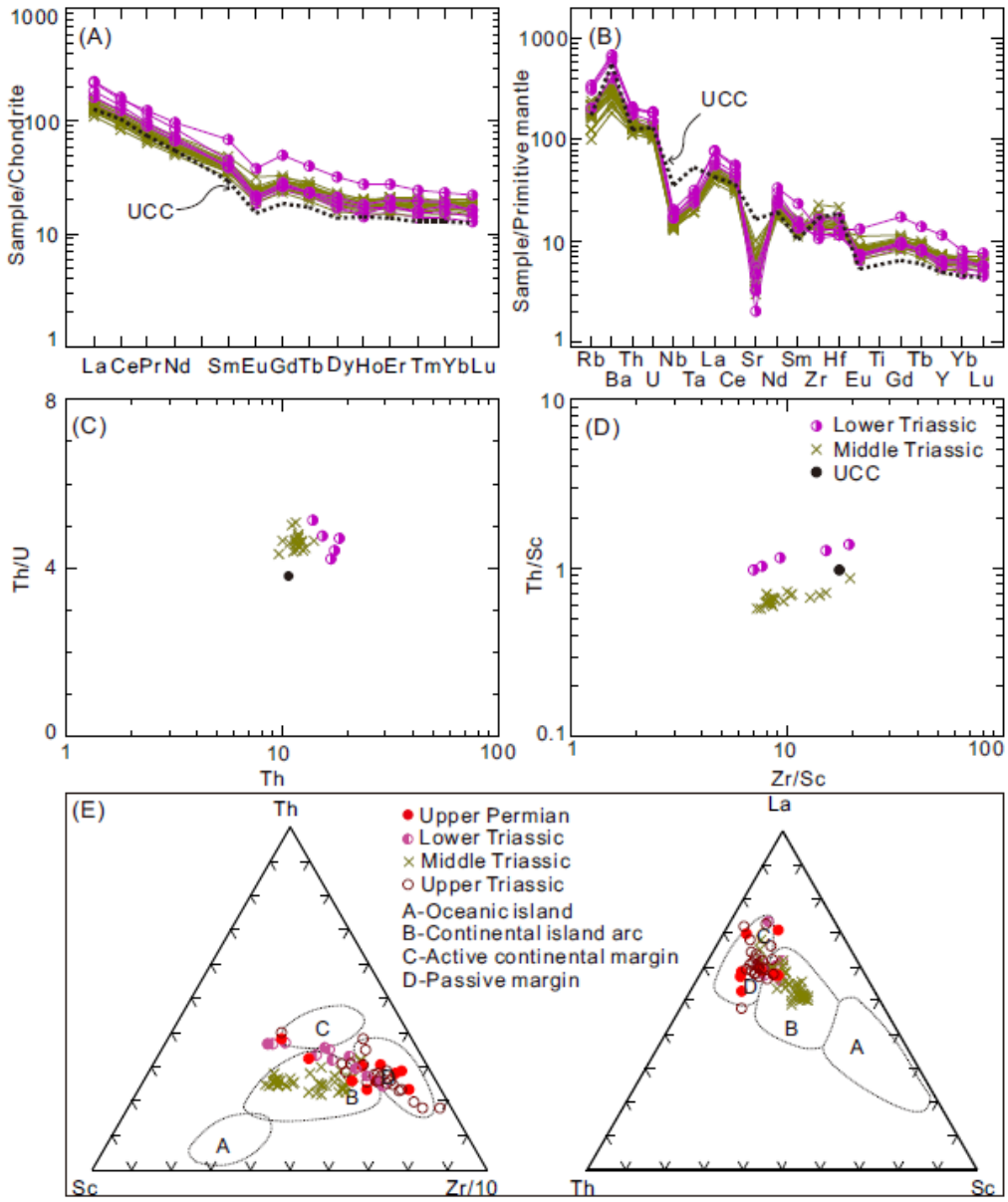

Figure 7

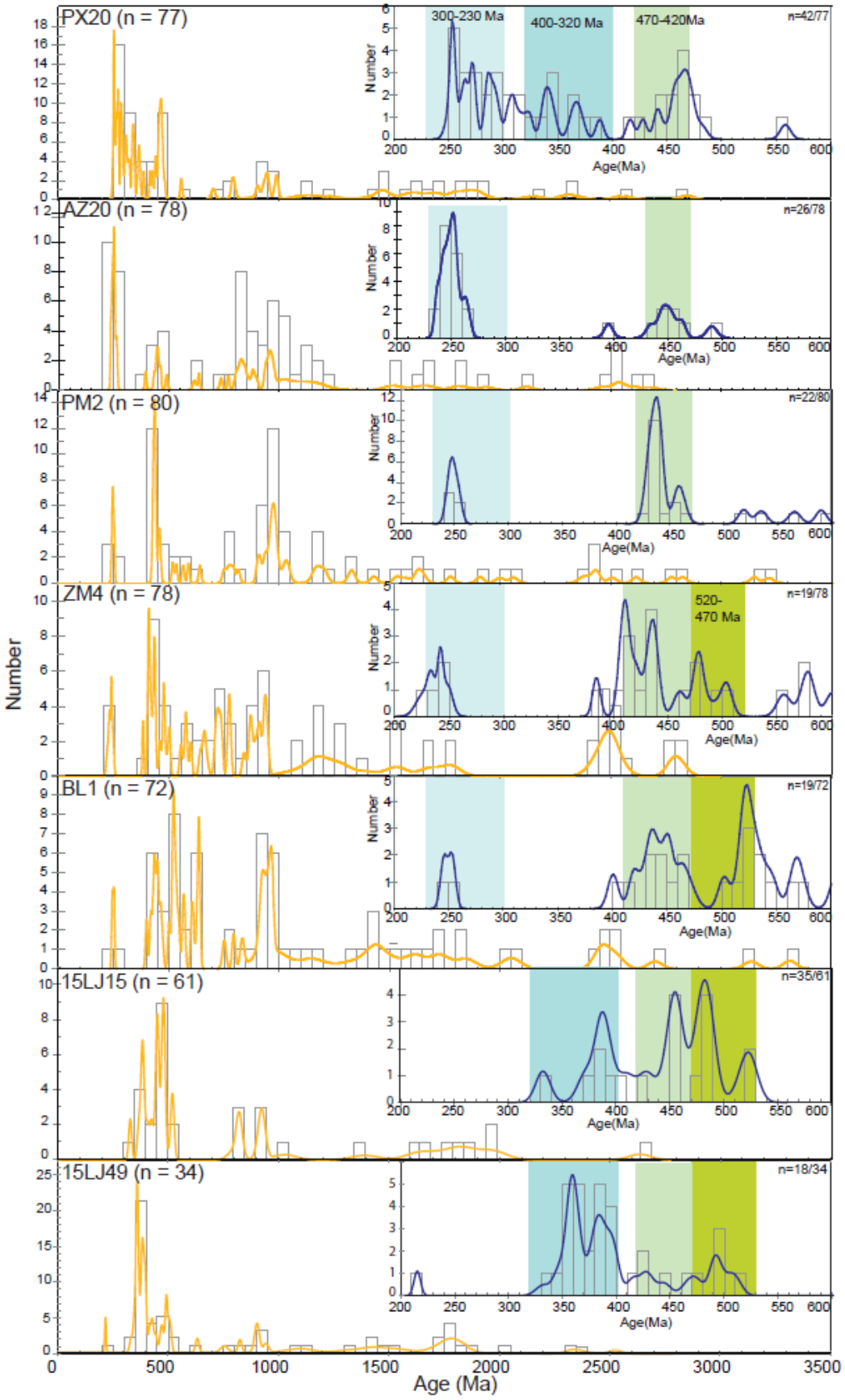

Figure 8

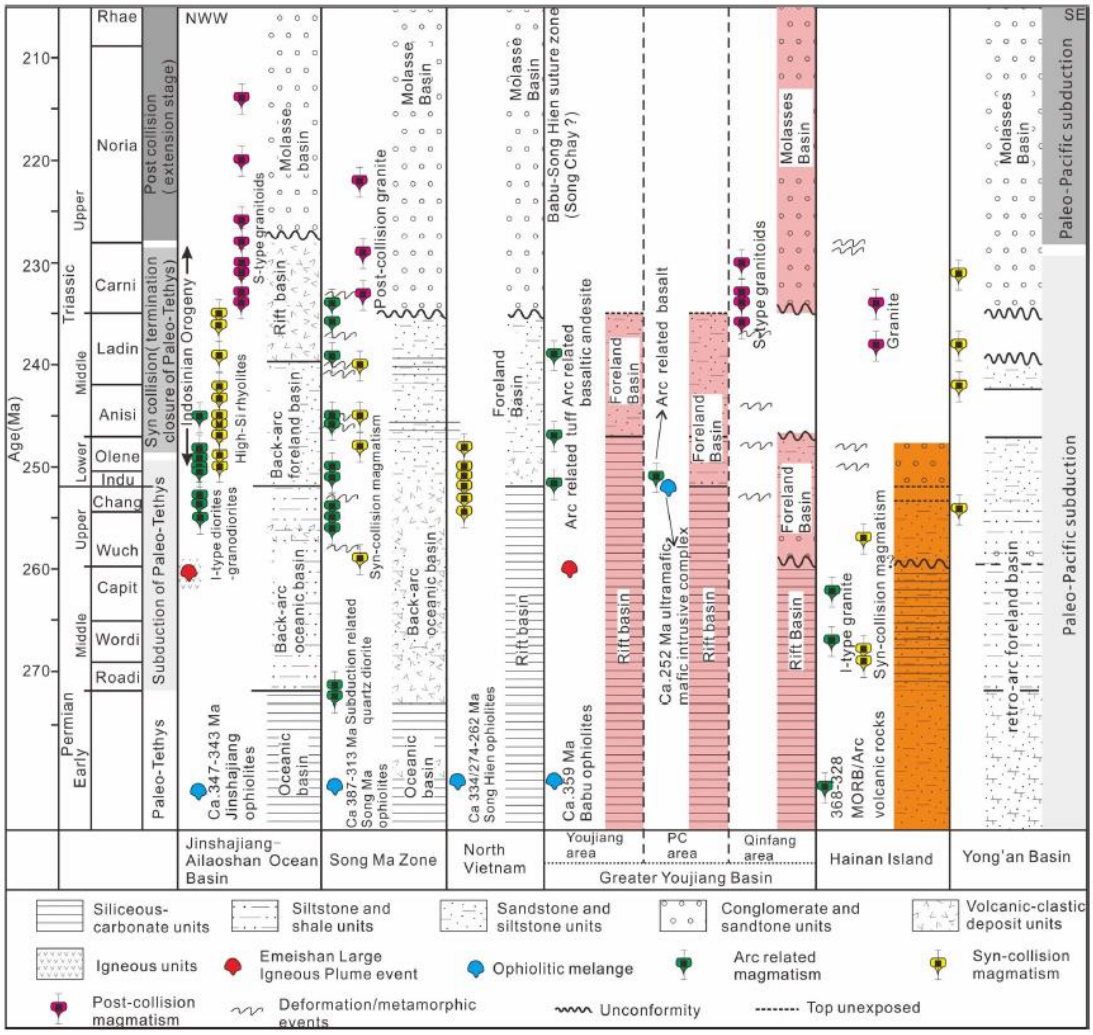

Figure 9

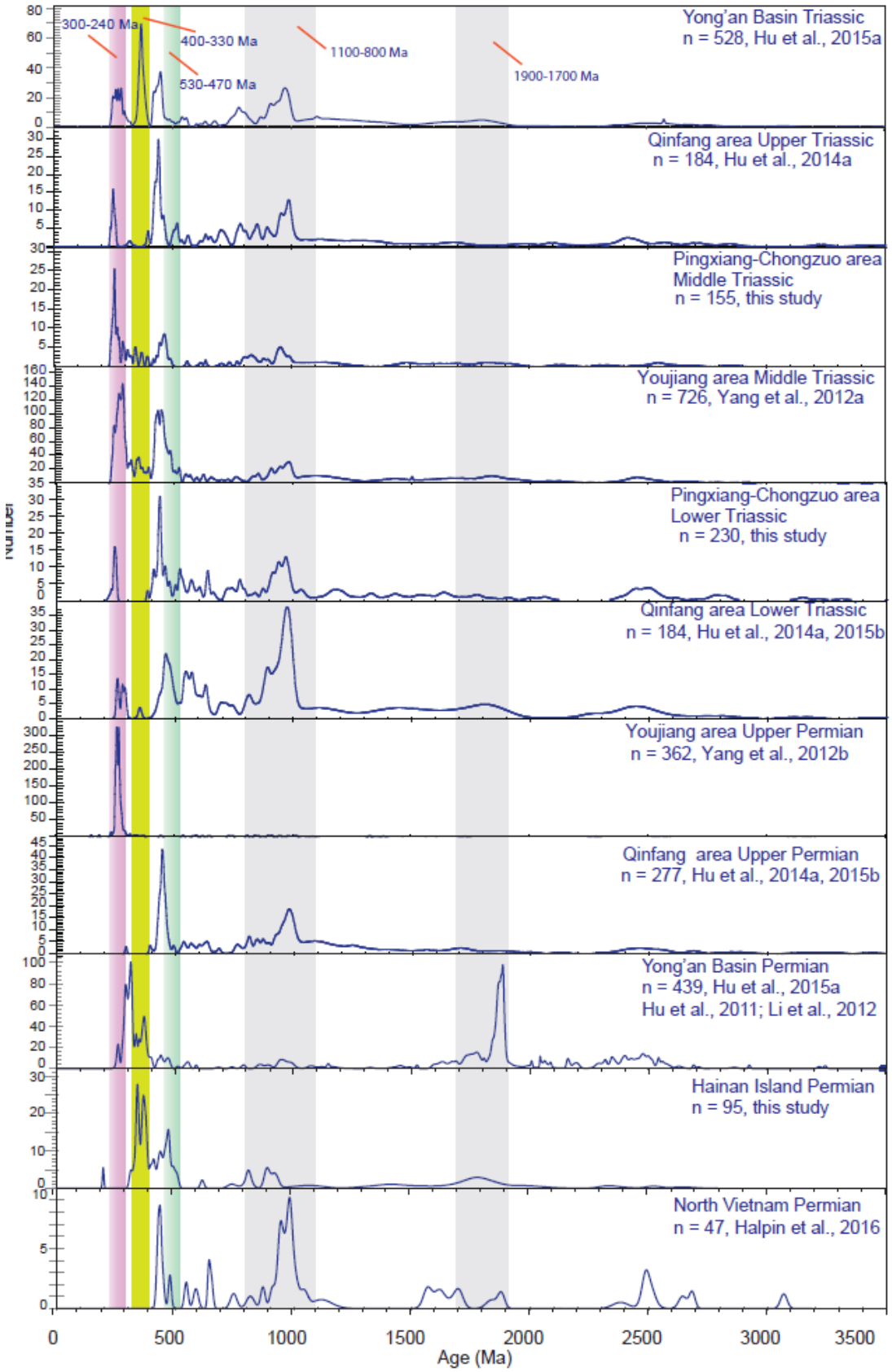

Figure 10

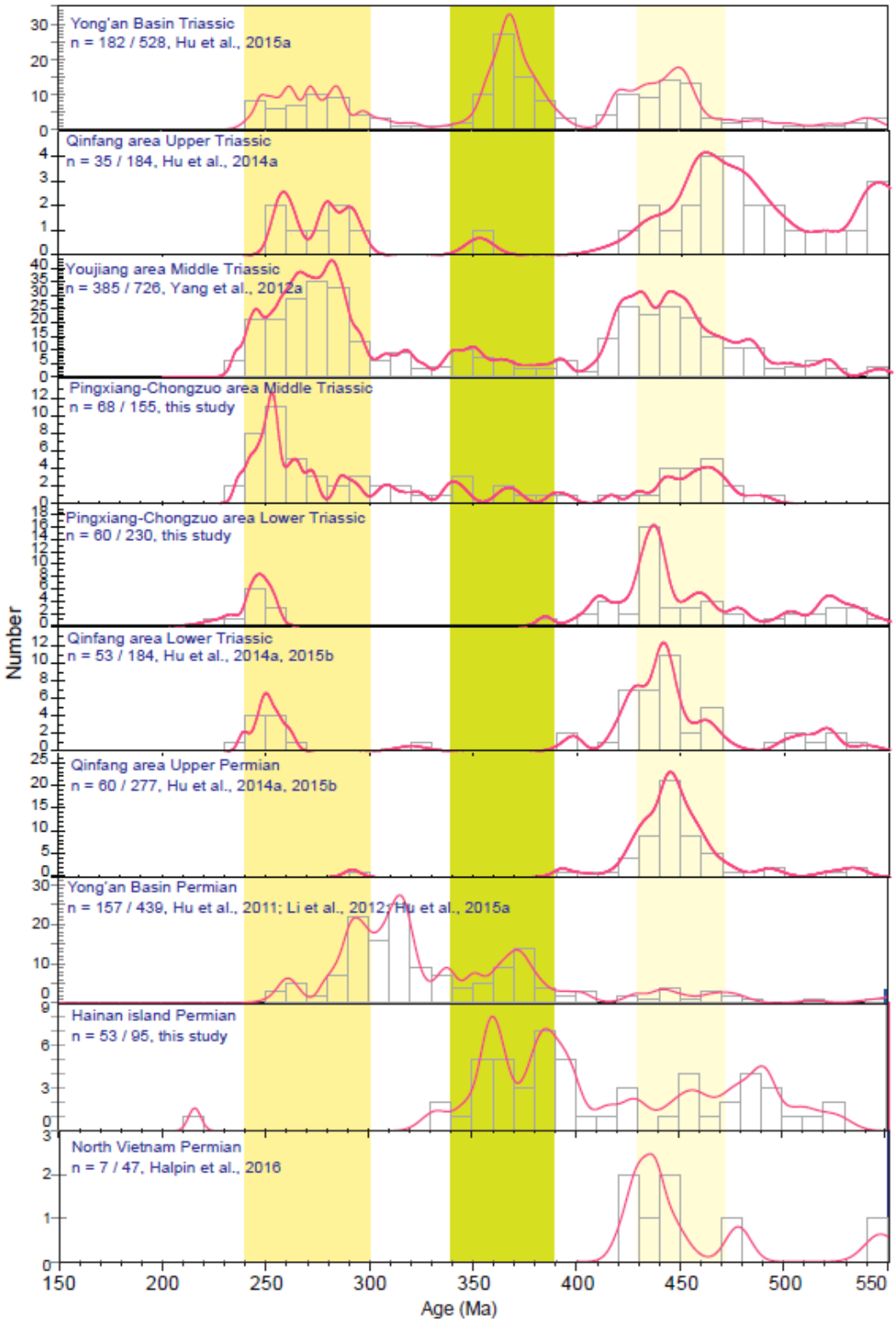

Figure 11

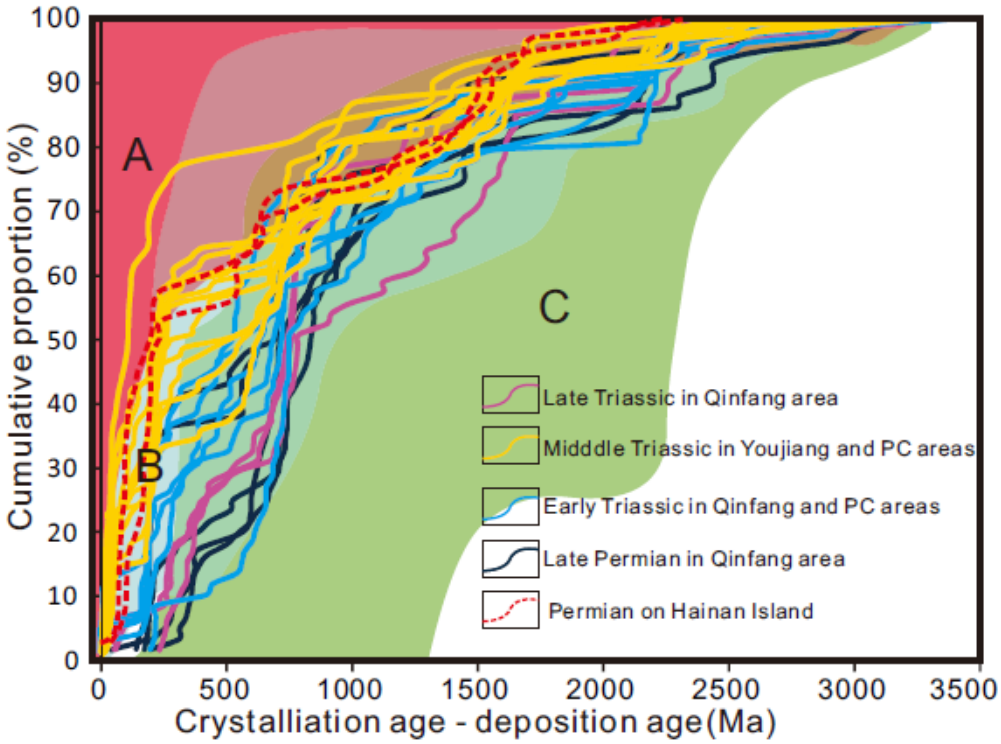

Figure 12

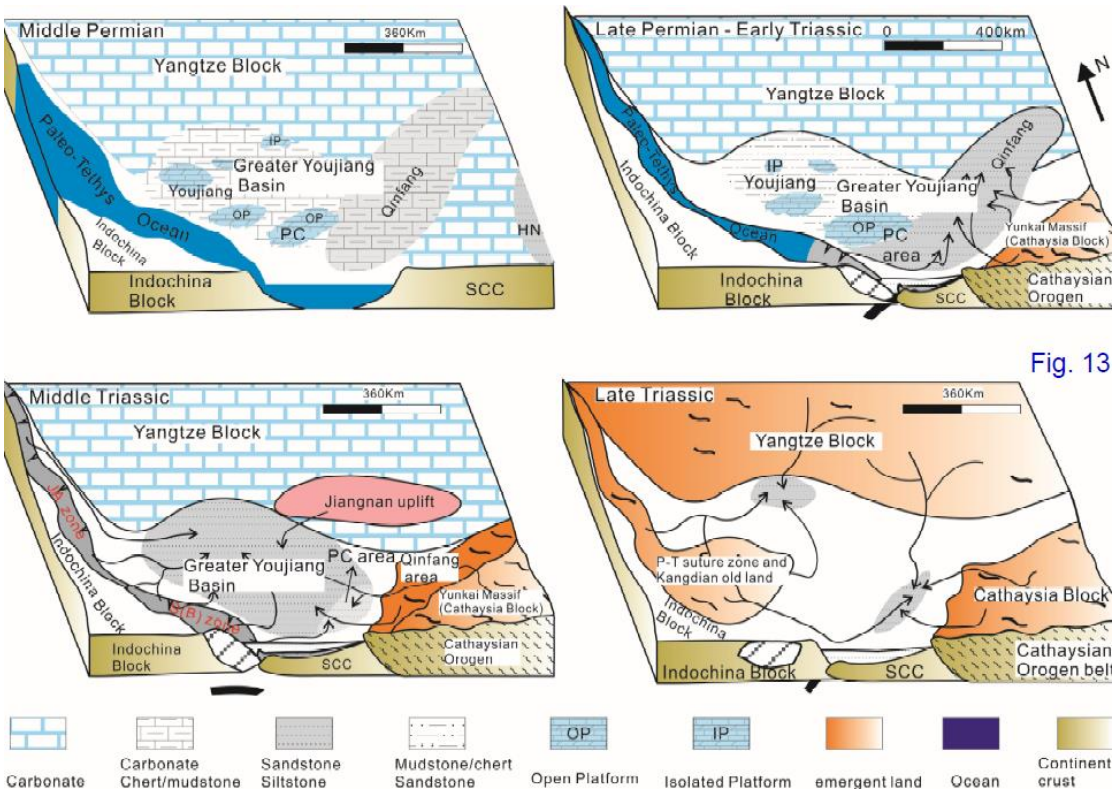

Figure 13

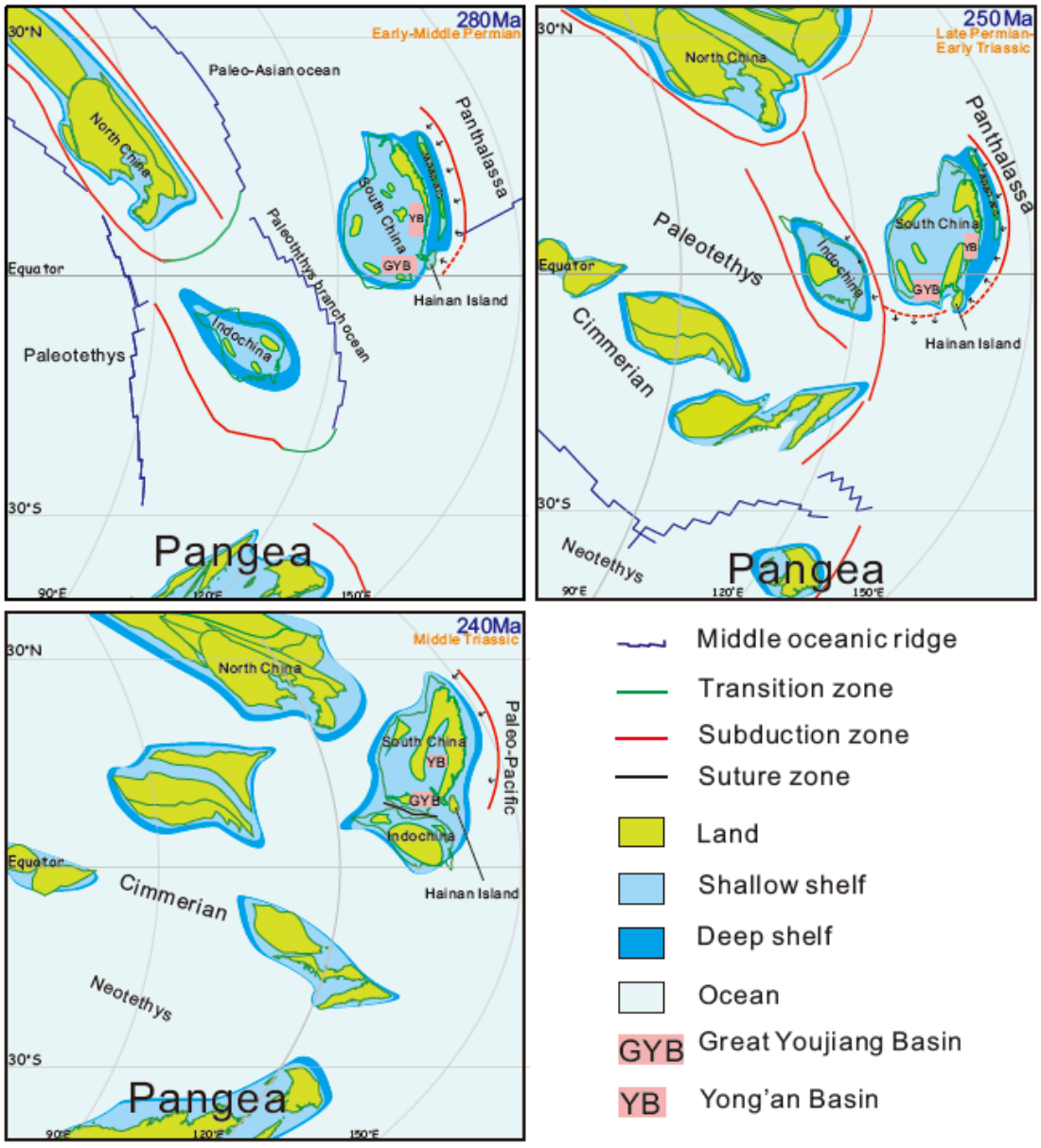

Figure 14

Highlights

1. Different source records in Hainan Island and Greater Youjiang Basin in Permian and Triassic, respectively.
2. Greater Youjiang Basin converted from trailing edge passive margin to peripheral foreland basin in Late Permian-Triassic
3. Oblique southeast to southwest between South China and Indochina blocks
4. Hainan Island constitute the southwest part of Paleo-Pacific Ocean subducted arc suture zone in late Paleozoic-Mesozoic